04 May 2006

Simulations of a New Continuous Steelmaking Process

Jorg Annie Peter

Kent D. Peaslee
Missouri University of Science and Technology, kpeaslee@mst.edu

D. G. C. Robertson
Missouri University of Science and Technology, davidrob@mst.edu

Simulations of a New Continuous Steelmaking Process

Jörg Peter
Kent D. Peaslee
David G. C. Robertson

University of Missouri-Rolla
Department of Materials Science and Engineering
1870 Miner Circle
218 McNutt Hall
Rolla, MO 65409-0340
Tel.: 573-341-4714
Fax: 573-341-6934
E-mail: jjpeter@umr.edu or kpeaslee@umr.edu

Keywords: continuous steelmaking, dynamic chemistry and temperature simulation, kinetics, refining, yield, carry-over slag

ABSTRACT

A new continuous steelmaking process has been designed in an effort to reduce meltshop costs and increase productivity beyond the possibilities of current EAF-LMF-CC meltshops. This paper discusses possible operational performance based on industrially-verified kinetic, thermodynamic, and heat-transfer models. Dynamic simulations predict variations in steel chemistry and temperature, resulting from steel treatment and upsets. Savings in costs are projected because of increased metallic yield, lower energy requirements, more efficient use of deoxidants and alloys, fewer man-hours per ton, and decreased capital investment.

INTRODUCTION

Chemical and thermal performances of a new continuous steelmaking process are investigated in this paper. The proposed process was introduced in a previous publication[1], including the design and functions of each reactor and several steady-state simulations. The calculated simulations and predictions of the previous publication and of this document are based on models that were verified with industrial data[2].

The change over time of steel chemistry and temperature during continuous operation with varying parameters will be explained with the help of specific examples. These examples include:

- an abrupt sulfur increase and the associated corrective action to maintain the required final sulfur concentration,
- a grade change, decreasing the manganese concentration by one half without increasing the amount of intermix material as compared to current operations,
- a heat loss study to predict the required steel temperature in the Electric Arc Furnace (EAF) for production (flow) rates that range between 30 t/hr and 200 t/hr,
- a simulation of the heat losses and the required steel temperatures during start-up operation,
- and a comparison of these heat losses to heat losses during current operations, producing 165 t/hr with three 124-ton ladles using a Ladle Metallurgy Furnace (LMF).

This paper concludes with an estimation of the potential savings by operating the new continuous process as compared to current EAF-LMF steelmaking practices.

Process overview
Figure 1 shows the five interconnected vessels of the new process. Steel will continuously flow through this system while it is being treated. Preheated scrap will be continuously charged and melted in the first vessel (modified AC Consteel® EAF). Melting will be accomplished with electrical and chemical energy while maintaining a foamy slag and performing preliminary de-C and de-P. Additional de-C and de-P will be achieved in the second vessel (Oxidizer). Near-equilibrium conditions allow for a partial de-O of the steel in the Oxidizer, depending on the required final carbon concentration. In the third vessel (Reducer), steel will be continuously de-O, de-S, and alloyed. The cone-shaped Reducer is designed to achieve high mass transfer rates and therefore a low final sulfur concentration while maintaining high production rates. The operations in the fourth vessel (Finisher) will include additional de-S and alloy additions, inclusion floatation, and homogenization before the steel will flow into the fifth vessel (Tundish).

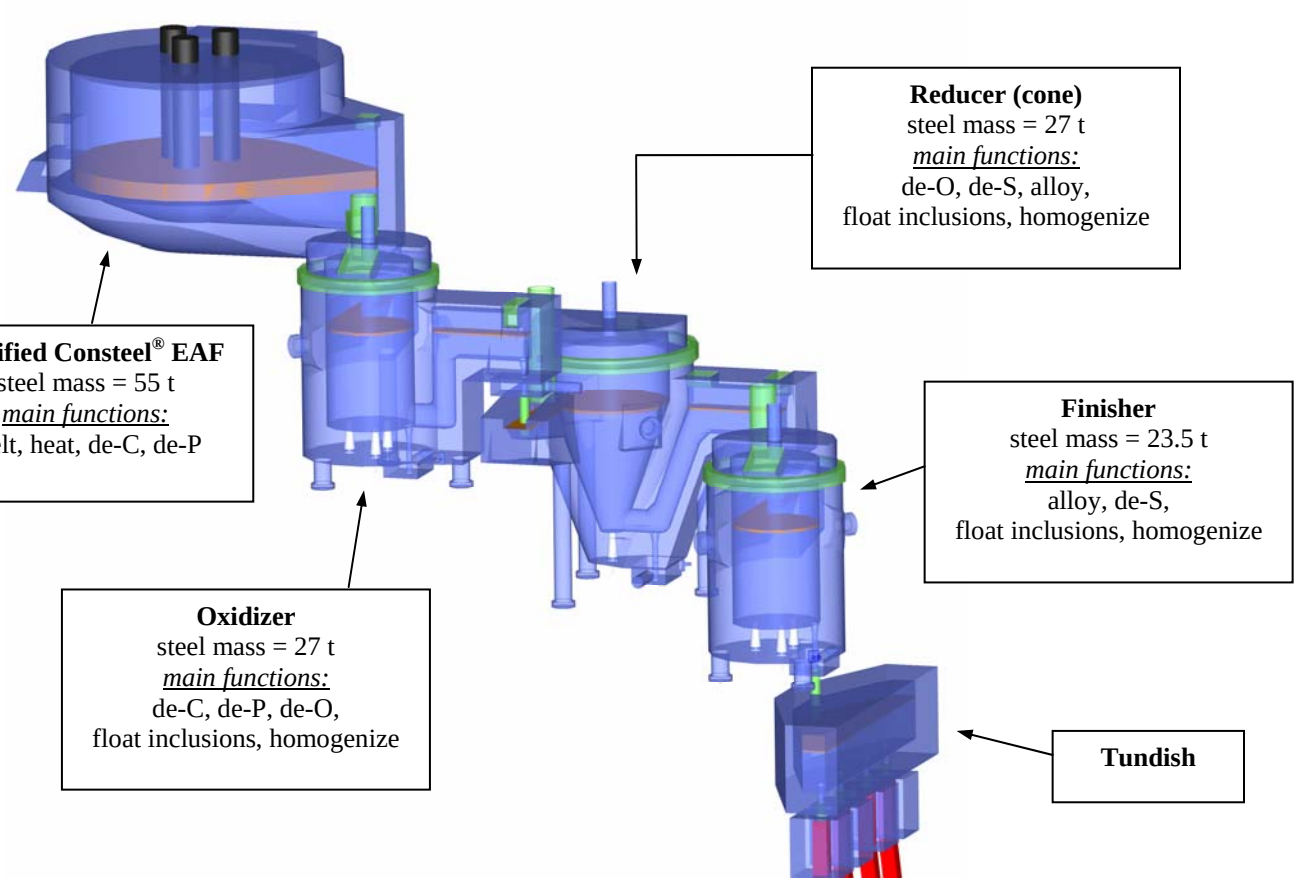

Figure 1: Side view of the vessels of the continuous steelmaking process

PREDICTION OF OPERATIONAL PERFORMANCE

Dynamic Metsim model for steel treatment in continuous refining vessels
The effects of increasing the sulfur concentration and changing grades were simulated; using a computer model constructed with Metsim, a commercial software package capable of performing dynamic simulations of a multitude of processes. The model was designed to simulate the successive refining in the three continuous refining vessels (Oxidizer, Reducer, and Finisher) similar to the model that was developed for ladle treatment[2]. The model of each continuous refiner was modified to allow steel to continuously flow through the simulated system of interconnected vessels.

The production (flow) rate, the EAF steel compositions, the feeding rates and types of fluxes and alloys, as well as the argon flow rates are inputs to the model. The steel and slag composition in each refining vessel (Oxidizer, Reducer, and Finisher) and the slag amount as a function of time are the calculated results of the simulations. The steel and slag compositions that exit each vessel have the same composition as the steel and the slag that are in the vessel. It is assumed that each vessel closely resembles a near-equilibrium Completely Stirred Tank Reactor (CSTR) based on fluid flow simulations[3] that were verified with industrial data[4].

The simulation of each refining vessel requires a value of the mass transfer rate constant. This value represents the fraction of the steel that reacts with the slag during a specific period. The concentrations of steel components change during refining according to Equation 1 (first-order rate equation) if the equilibrium concentrations at the slag/steel interface stay constant. However, thermodynamic conditions change over time during actual operation. Therefore, the equilibrium concentration of each steel component is assumed to be constant for only 10 seconds (one time step) during the Metsim computations. In addition, the design of the Metsim model, as illustrated in Figure 2, ensures that all steel and slag components are influenced by the mass transfer rate constant during the simulations. Equation 1 is only written for one steel component.

$$\frac{dC}{dt} = -k\left(C - C_{equ}\right) \tag{1}$$

Explanation of symbols in Equation 1:
C = instantaneous concentration of one steel component
C_{equ} = equilibrium concentration of steel components at the slag-steel interface
d = differential operator
k = mass transfer rate constant
t = time

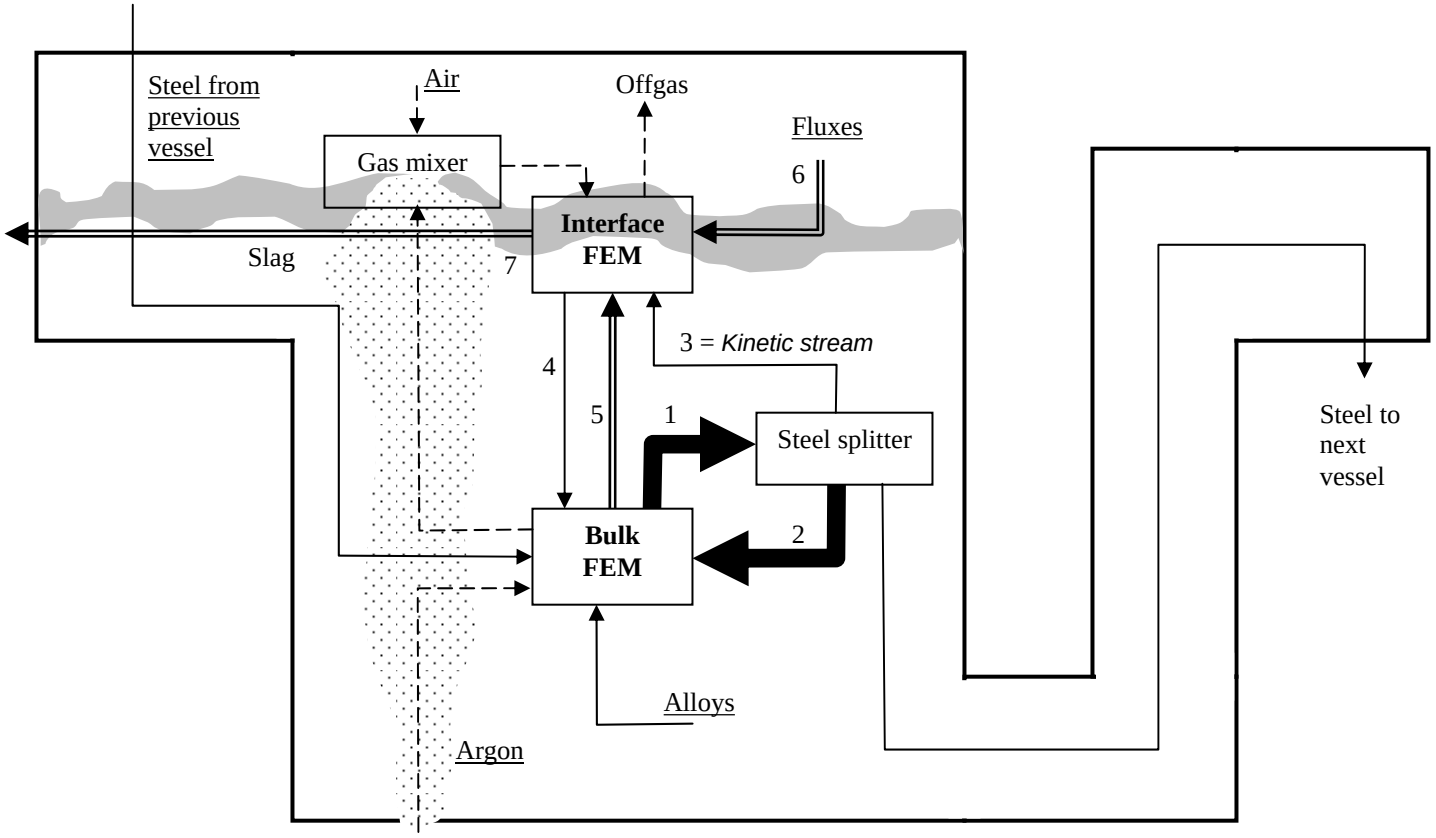

Figure 2: Illustration of Metsim model used for simulation of steel treatment in each of the three continuous refining vessels

Figure 2 shows the Metsim model of one continuous reactor. Free Energy Minimizer (FEM), mixer, and splitter modules as well as streams were used to create three identical continuous Metsim models, one for each of the three continuous refining vessels. Streams allow for material flow among the modules of one refining vessel and for the flow of steel between the three connected Metsim models that represent the Oxidizer, Reducer, and Finisher.

The slag/steel reactions were calculated with the Interface FEM and the reaction within the steel were calculated with the Bulk FEM. The pressures in these FEM's were set at 1.0 atm and 1.3 atm respectively. The chosen values of activity coefficients of elements and compounds are based on verified Metsim simulations of steel treatment in 125-ton and 150-ton ladles[2]. The simulations were verified with industrial data and included thermodynamical calculations with FactSage.

Steel from the previous vessel mixes and reacts with the steel of the current vessel in the Bulk FEM. The wide, solid streams 1 and 2 in Figure 2 represent the bulk flow of the steel that does not react with the slag during one calculation. The width of these streams indicates that the majority of the steel does not react with the slag during each calculation. The flow rate of stream 1 is the quotient of the steel mass in the vessel and the time step (10 sec). The flow rate of returning stream 2 is the flow rate of stream 1 reduced by the flow rate of the kinetic stream 3 and the steel that flows to the next vessel. Steel is transported to the Interface FEM by the kinetic stream 3 while it returns to the Bulk FEM through stream 4.

The flow rate of the kinetic stream 3 is the product of the steel mass in the vessel and the mass transfer rate constant. The value of the mass transfer rate constant is paramount for the chemical performance of each continuous refining vessel. For that reason, current industrial steel-treatment operations were studied in detail[2] to correlate the value of the mass transfer rate constant to measurable operational parameters. The result of this study[2] is summarized with Equation 2, which was used to determine the mass transfer rate constants for the simulations of the continuous refining vessels. The value of the proportionality constant in Equation 2 was corrected from 0.08 (previous publication[2]) to 0.073 after a reevaluation of the data. The mass transfer rate constant depends on the argon flow rate, the shape and size of the reactor, as well as on the prevailing pressure and temperature.

$$k = \frac{0.073}{m}\sqrt{14.23\frac{QTA_{top}}{N^{1/4}}\log_{10}\left(1+\frac{h}{1.5P_o}\right)} \qquad (2)$$

Explanation of symbols in Equation 2:
A_{top} = nominal top area of steel slag interface m^2
h = steel height in m
k = mass transfer rate constant in min^{-1}
m = Steel mass in metric tons
N = number of porous plugs
P_o = ambient pressure above the bath in atm
Q = argon flow rate in Nm^3/min
T = steel temperature in kelvin

Streams that carry oxides or other non-metallic components are represented by double lines in Figure 2. Stream 5 allows inclusions to travel from the Bulk FEM to the Interface FEM. Fluxes are supplied to the Interface FEM by stream 6. Stream 7 represents the resulting slag that continuously flows out each vessel. Alloys are entered into the Bulk FEM. Dashed lines in Figure 2 represent gas streams. Argon enters the Bulk FEM and the product gas of the Bulk FEM is mixed with entrained air. The resulting gas mixture reacts in the Interface FEM and leaves the system as offgas.

Steady-state operational parameters and performance

Current steel treatment in the ladle is most efficient if standardized operations are practiced, ensuring that the aim chemistry is consistently met at the end of the ladle treatment. Steel treatment during the continuous operations of the new process would ensure that the chemistry in the Finisher is consistently at the final aim chemistry. The steel compositions of the other continuous reactors are also at their required aim compositions. The calculated changes during dynamic simulations of upsets in the continuous reactors over time will be explained in respect to the conditions, parameters, and results of a 165 t/hr steady-state production.

The calculated steady-state concentrations of major steel components (C, Mn, P, S, Si) in the EAF, Oxidizer, Reducer, and Finisher as well as the steel temperatures, amount and type of alloy additions, argon flow rates, and the EAF energy requirements are summarized in Figure 3. The electricity and oxygen consumptions are based on current Consteel® operations[5]. The steel temperatures are based on thermal calculations explained later in this paper. The argon flows relate to the mass transfer rate constants according to Equation 2. The EAF carbon concentration of 0.08% corresponds to 14% FeO in the slag due to constant near-equilibrium conditions in the furnace. It is believed that the metallic yield in the EAF could be maintained at 95%. The relatively high EAF carbon concentration would be decreased to 0.05% in the Oxidizer due to hematite and bauxite additions. The carbon increase in the Reducer is caused by the carbon in the SiMn alloy. The EAF phosphorus concentration is expected to be 0.010%. It would decrease in the Oxidizer to 0.004% before additional phosphorus would be added in the Reducer with the SiMn. Most of the sulfur would be removed in the Reducer, achieving a reduction from 0.050% to 0.015%. Additional de-S in the Finisher would result into a final sulfur concentration of 0.008%. SiMn and FeSi are added in the Reducer, ensuring a final composition of 0.90% Mn and 0.25% Si. Other alloys such as FeV could be added in the Reducer or, as listed in Figure 3, in the Finisher. The compositions of the alloys and fluxes used during the steady-state and dynamic simulations are listed in Table I.

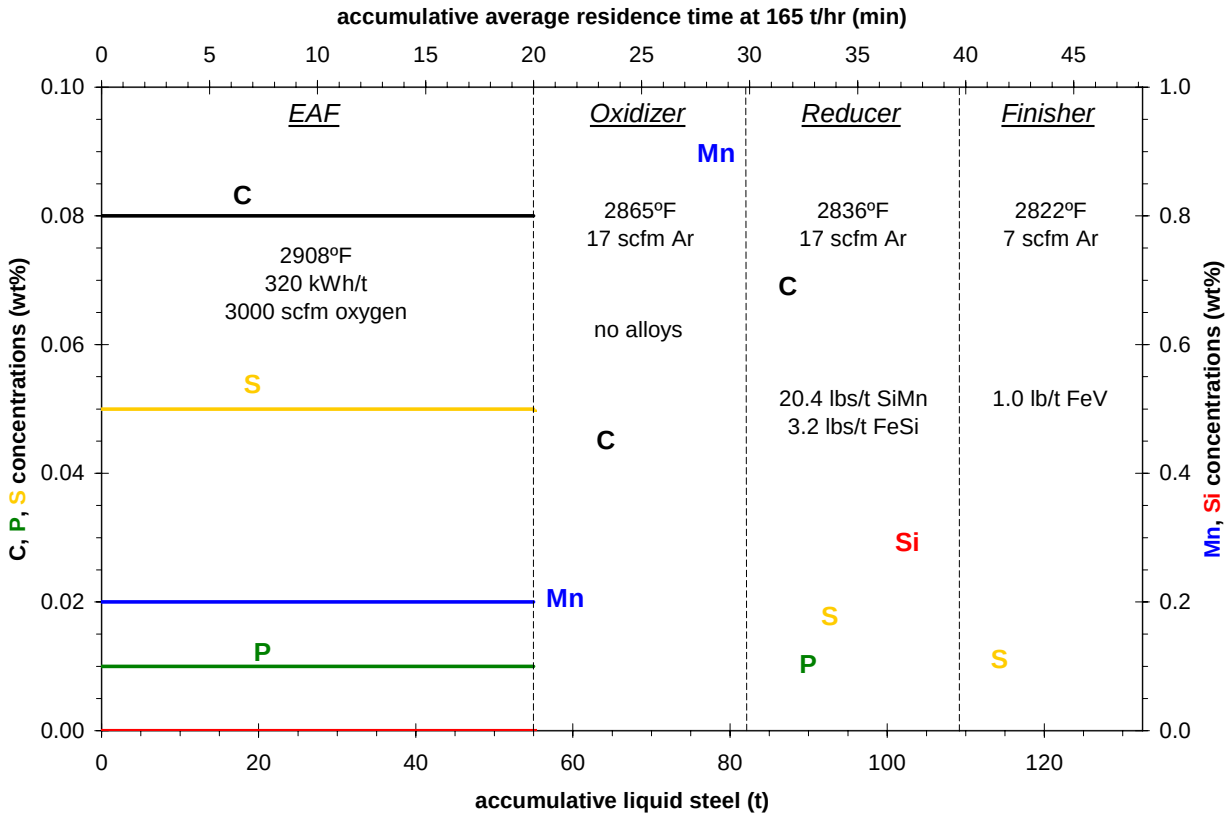

Figure 3: Metsim-calculated steady-state steel chemistry (C, Mn, P, S, Si) and operation conditions (temperature, argon flow rate, energy) at steady production (flow) rate of 165 t/hr in the continuous steelmaking reactors (EAF, Oxidizer, Reducer, Finisher)

Table I: Major components of alloys and fluxes that were used to simulate the performance of the continuous steelmaking process

Alloys				
wt%	C	Mn	P	Si
HC-FeMn	7	77	0.3	1
MC-FeMn	1.3	81	0.2	1
SiMn	1.8	71	0.4	18
FeSi	0.1	0.3	0.02	75

Fluxes					
wt%	CaO	SiO_2	Al_2O_3	MgO	Fe_2O_3
Lime	96	1.2	1	1.5	0.3
Dolomitic lime	59.5	0.5	0.2	39.5	0.3
Calcium-aluminate	30	7	42	20	1
Bauxite	2	7	60	1	30
Hematite	-	6	2	-	92

Steady-state compositions and amounts of the slags in the EAF, Oxidizer, Reducer, and Finisher together with the flux additions that correspond to the steel chemistries of Figure 3 are elucidated in Figures 4 through 6. These figures contain phase diagrams that were calculated with FactSage at the displayed temperatures and compared to published phase diagrams that are based on measurements, finding good agreement. The phase "slag" in these phase diagrams refers to compositions at which the entire slag is liquid. Lines indicate saturations limits or liquidus lines of the listed solids. The name of the solid (e.g. MgO) refers to a solid solution in which the named compound predominates. If several lines are between the liquid slag and the composition of interest, then all the solid solutions associated with these lines are present. The phase diagrams are labeled up to 100%; however, 100% corresponds to total concentration of the three compounds that are listed on the corners of each phase diagram. The total concentrations of these three compounds are listed in the captions in each figure and range between 78% and 83% of the actual slag composition. The concentrations of the components that are constant at all points in the phase diagram can be obtained from the lists next to the phase diagrams.

The composition of the EAF slag is listed and marked in the CaO-SiO_2-Al_2O_3-MgO-MnO-FeO-P septenary phase diagram in Figure 4. The slag contains 4 wt% solid magnesiowüstite to promote a stable foamy slag and to minimize slag line corrosion. A V-ratio [$CaO/(SiO_2+Al_2O_3)$] of 1.6 corresponds to a liquidus magnesiowüstite line that is nearly perpendicular to the CaO-SiO_2 axis and points to the FeO corner. As a result, the steady-state, near-equilibrium FeO concentration of the slag can be varied based on the CO/CO_2 ratio in the furnace while the required amount of solid particles is maintained, making it possible to maintain a high yield.

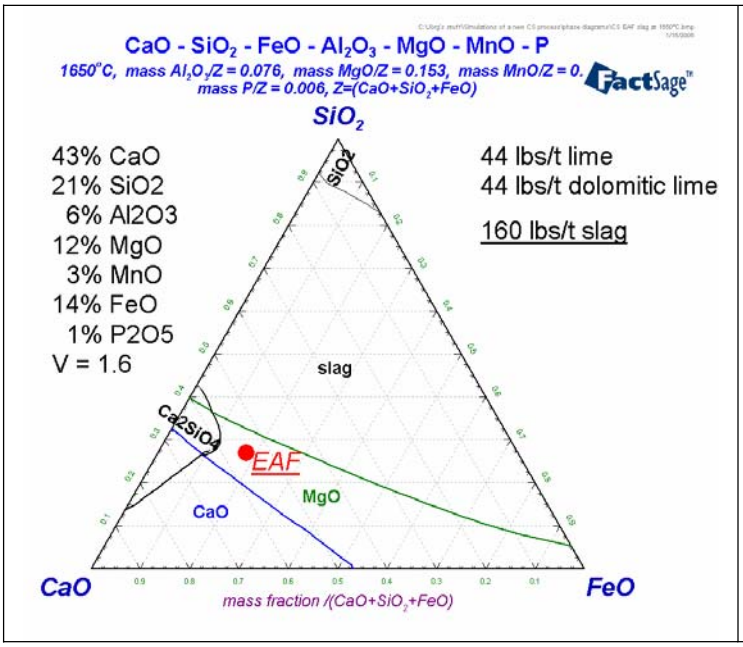

Figure 4: The **EAF** slag is mapped on a CaO-SiO_2-Al_2O_3-MgO-MnO-FeO-P septenary phase diagram at 3002ºF. (Steel temperature is 2908ºF.) The sum of **CaO, SiO_2 and FeO is 78%** of the total slag. The displayed composition refers to marked, red point. Amounts of slag additives and slag amount are listed. The steel production (flow) rate is 164 t/hr.

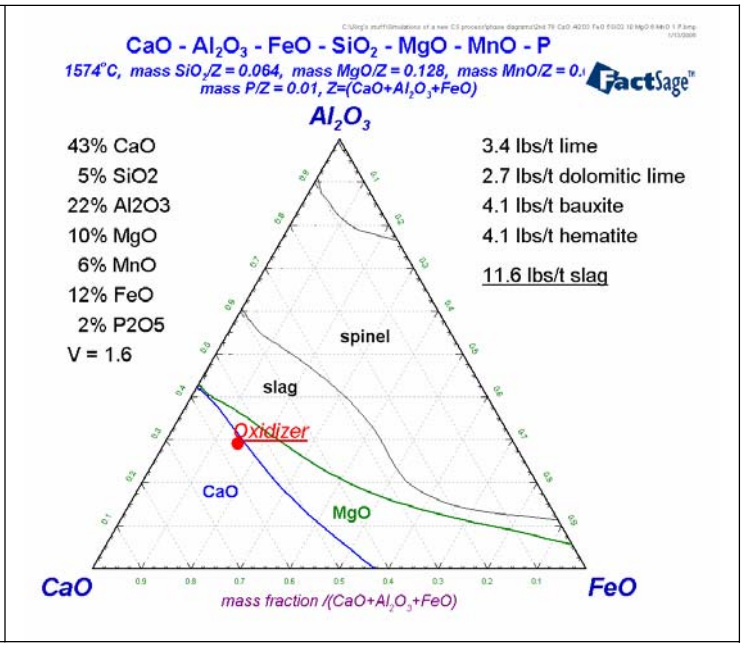

Figure 5: The **Oxidizer** slag is mapped on a CaO-SiO_2-Al_2O_3-MgO-MnO-FeO-P septenary phase diagram at 2865ºF. The sum of **CaO, Al_2O_3 and FeO is 78%** of the total slag. The displayed composition refers to marked, red point. Amounts of slag additives and slag amount are listed. The steel production (flow) rate is 164 t/hr.

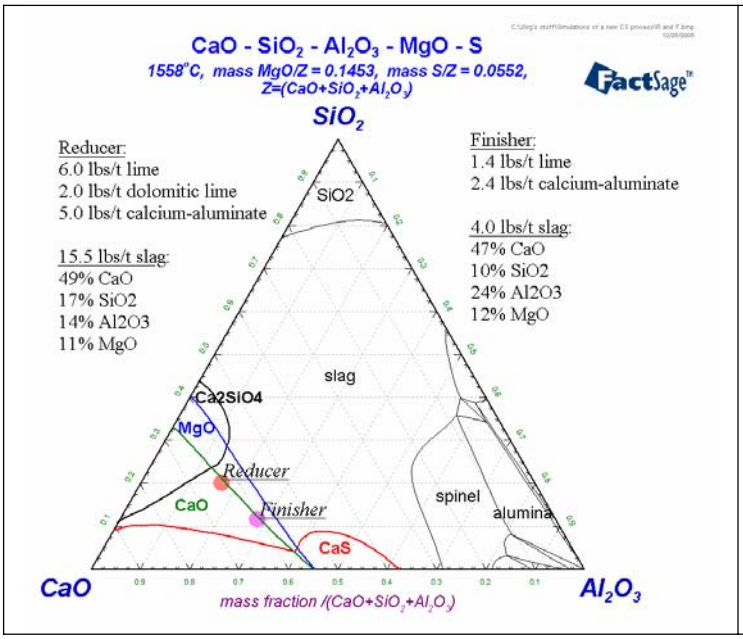

Figure 6: The **Reducer and Finisher** slags are mapped on a CaO-SiO_2-Al_2O_3-MgO-S quinary phase diagram at 2836ºF. The sum of **CaO, SiO_2 and Al_2O_3 is 83.3%** of the total slag. The displayed compositions refer to marked points. Amounts of slag additives and slag amounts are listed for both slags. The average sulfur concentration is 4.6%. The MgO averages 12.1%. The steel production (flow) rate is 165 t/hr.

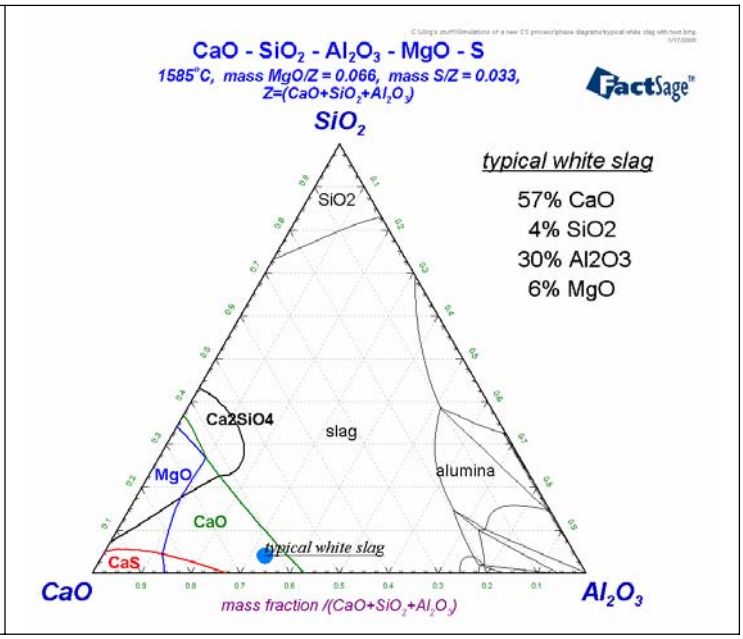

Figure 7: A **typical white slag** at the end of a common ladle treatment is mapped on a CaO-SiO_2-Al_2O_3-MgO-S quinary phase diagram at 2885ºF. The sum of **CaO, SiO_2 and Al_2O_3 is 91%** of the total slag. The displayed composition refers to marked, blue point. The sulfur concentration of the slag is 3%.

The $CaO-SiO_2-Al_2O_3$-MgO-MnO-FeO-P septenary phase diagram in Figure 4 compares well to a plane that cuts through the three-dimensional quaternary CaO-FeO-MgO-SiO2 phase diagram at 12% MgO in Figure 147 in the Slag Atlas[6]. The phase diagram in Figure 4 could also be compared to the quaternary $CaO-MgO-SiO_2$-FeO phase diagrams published by Turkdogan[7]. The effect of MnO on the $CaO-SiO_2$-FeO system is reported in the same publication[7].

The composition of the Oxidizer slag is listed and marked in the $CaO-SiO_2-Al_2O_3$-MgO-MnO-FeO-P septenary phase diagram in Figure 5. The slag is saturated with 2 wt% solids, containing mainly MgO to minimize slag line corrosion. The high Al_2O_3 concentrations (22%) and low SiO_2 concentration (5%) as compared to the furnace slag increases the activity coefficient of the FeO. The slag composition of the Oxidizer, the constant, near-equilibrium conditions, and the argon stirring through three porous plugs allow for the calculated decrease of the carbon and phosphorus concentrations beyond the refining in the EAF. This procedure makes high carbon concentration and metallic yield in the EAF possible in addition to a low phosphorus concentration in the final product. The septenary phase diagram in Figure 5 compares well to the ternary $CaO-Al_2O_3-Fe_3O_4$ phase diagrams in Figure 5094 in Phase Diagrams for Ceramists[8].

The compositions of the Reducer and Finisher slags are listed and marked in the $CaO-SiO_2-Al_2O_3$-MgO-S quinary phase diagram in Figure 6. The slags are saturated with 2 wt% solids, containing mainly MgO to minimize slag line corrosion. There is more slag produced in the Reducer (15.5 lbs/t) than in the Finisher (4.0 lbs/t) because more fluxes need to be added in the Reducer due to greater production of SiO_2 and due to greater transfer of sulfur from the steel into the slag in the Reducer as compared to the Finisher. The SiO_2 concentration is higher in the Reducer slag than in the Finisher slag because the steel is deoxidized with silicon in the Reducer. The slag sulfur concentrations, sulfide capacities, and sulfur distribution ratios in the Reducer and Finisher are 4.3% and 3.1%, 0.022 and 0.015, 290 and 414 respectively. The values are higher in these slags as compared to typical ladle slags. Peter et al.[5] reported that these values could be increased for current ladle slags if ladle slags would be MgO-saturated and/or if the EAF carry-over slag would be decreased. The design of the new process makes it possible to minimize the amount of oxidized slag entering the Reducer and to minimize air entrainment[1]. In addition, constant low FeO concentrations (~0.02%) in the Reducer and Finisher slags minimize the transfer of oxygen from the atmosphere above the bath through the slag to the slag/steel interface. This oxygen source increases with increasing FeO concentration and it can be larger than the uptake of oxygen through the open eye[2].

The composition of a typical white slag at the end of a common ladle treatment is listed and marked in the $CaO-SiO_2-Al_2O_3$-MgO-S quinary phase diagram in Figure 7 for comparison. Most ladle slags are typically CaO but not MgO saturated. The masses of current ladle slag commonly range between 35 and 45 lbs/t[5] while the sum of the slag masses from Oxidizer, Reducer, and Finisher is 31 lbs/t.

The quinary phase diagram in Figure 7 resembles closely the quaternary phase diagram ($CaO-SiO_2-Al_2O_3$ with constant 5%MgO) in Figure 126 in the Slag Atlas[6] while the quinary phase diagram in Figure 6 resembles closely the quaternary phase diagrams ($CaO-SiO_2-Al_2O_3$ with constant 10% or 15%MgO) in Figures 127 and 128 in the Slag Atlas[6]. The sulfur concentration in the phase diagram in Figure 6 is higher (4.6%) than the sulfur concentration in the Reducer or Finisher at steady-state operation (4.3% and 3.1%) because it is an average that includes the sulfur concentrations in the slags with increased sulfur content (6.0% and 5.0%).

Simulations of a sulfur increase from 0.050% to 0.080% in the feed material

The performance of the process under changing conditions was simulated using an abrupt sulfur increase as an example. Figure 8 illustrates the calculated changes in sulfur concentrations in the steel of the EAF, Oxidizer, Reducer, and Finisher during a constant 165 t/hr production. The steady-state sulfur concentrations are plotted during the first 5 minutes. Hypothetical steel samples from the EAF and the Finisher were taken at the fifth minute, indicating to the operator that no changes occurred. However, at the same time the sulfur of the hypothetical incoming scrap increased from 0.050% to 0.080% or alternatively the sulfur content of the injected coal increased, causing the same effect. (A survey of eleven EAF operations showed that the EAF sulfur is only above 0.050% when high sulfur coal is used[5].) The sulfur increase was not detected for the next 30 minutes. The next hypothetical steel samples were taken at the 35th minute. The necessary analysis of the hypothetical samples delayed the start of corrective actions another 10 minutes until 40 minutes after the start of the abrupt sulfur increase (45th minute in Figure 8).

The sulfur increase is slow in all four reactors after the sulfur in the feed material significantly increased because the steel and slag in each continuous reactor are at the required, near-equilibrium compositions. The slowest increase occurs in the Reducer and Finisher because the steel was at the required chemistry before the upset, requiring time to be changed, and the sulfur is transferred from the steel into the slag at an increasing rate due to the slags' ability to hold a higher sulfur concentration than during initial steady-state operations. There is practically no increase in the sulfur concentration of the steel in the Finisher for the first 12 minutes after the increase of sulfur in the feed material. This time span exemplifies that continuous chemistry measurements (or more frequent sampling) would provide sufficient time to correct for upsets before any changes occur in the final steel that leaves the Finisher.

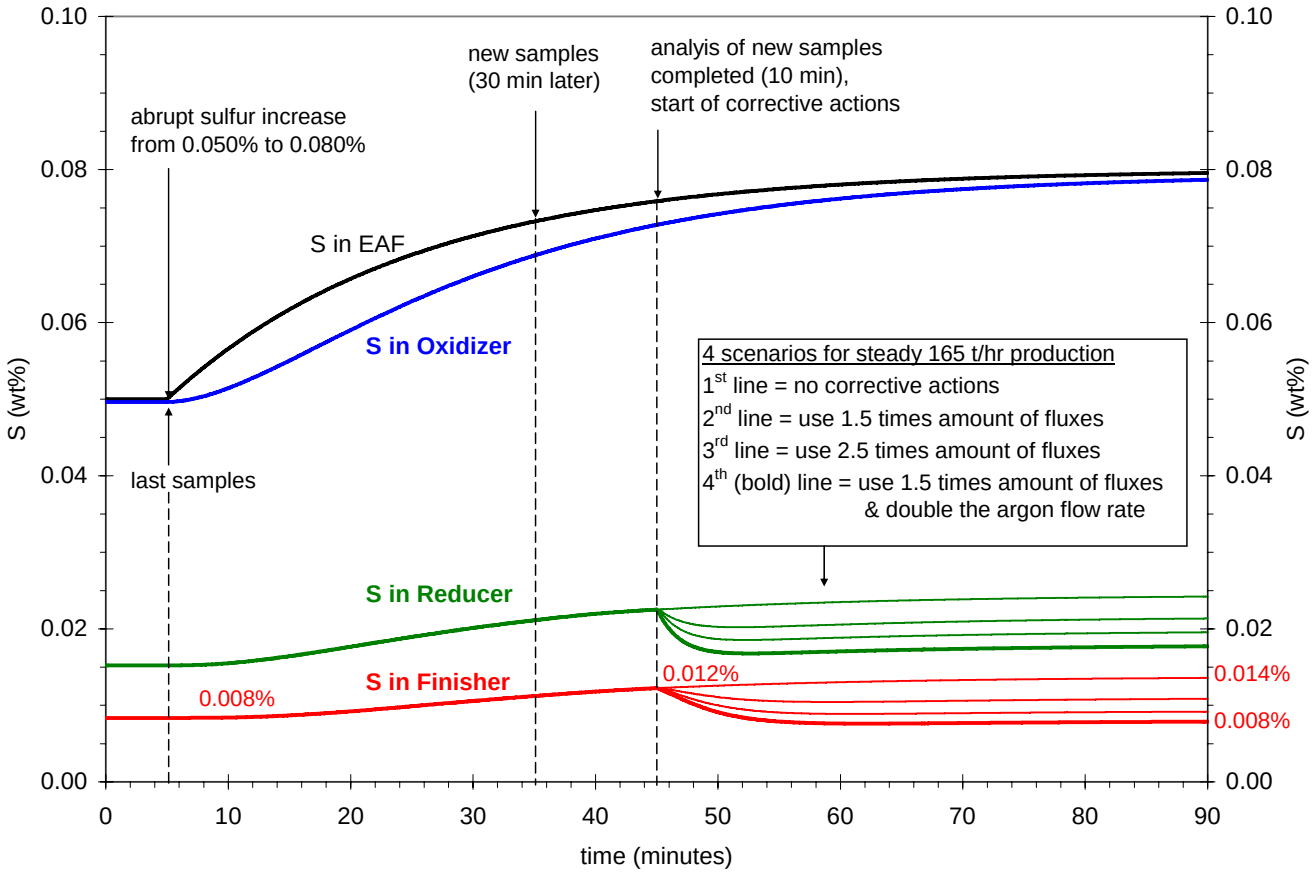

Figure 8: Simulation of an abrupt sulfur increase in the feed material and the resulting sulfur concentrations of the steel in EAF, Oxidizer, Reducer, and Finisher are illustrated, including the effects of corrective actions on the steel chemistry

The Metsim simulation demonstrated that the sulfur concentration in the Finisher would increase from 0.008% to 0.012% if no corrective actions were taken until 40 minutes after the abrupt sulfur increase in the feed material. At this time different corrective actions were simulated in an attempt to return to the initial 0.008% sulfur concentration of the steel in the Finisher. The sulfur concentration lines for the Reducer and Finisher in Figure 8 correspond to four different scenarios after the 45th minute:

1. The first set of lines or the lines with the highest sulfur concentrations show the simulations results if no corrective actions would be taken. The sulfur concentration of the steel in the Finisher would continue to increase until it reaches 0.014%.

2. The second set of lines with the second highest sulfur concentrations show the simulation results of a 50% increase in the flux feeding rates in the Reducer and Finisher as compared to the steady-state feeding rates reported in Figure 6. The sulfur concentration of the steel in the Finisher decreases only to 0.011%. This result is partly caused by the continued increase of the sulfur concentration of the steel that enters the Reducer.

3. The third set of lines with the third highest sulfur concentrations show the calculated results of a 150% increase in the flux feeding rates in the Reducer and Finisher as compared to the steady-state feeding rates reported in Figure 6. This simulation investigated the possibility of removing more sulfur from the steel by diluting the sulfur concentration in the slag. The large and costly increase of the flux feeding rates had only a small effect on the steel sulfur concentrations. The sulfur concentration of the steel in the Finisher decreased only an additional 0.002% to 0.009% as compared to the second scenario in which the increase of the flux feeding rates was significant smaller. This result indicates that the mass transfer and therefore the argon flow rates needed to be increased in order to return to the initial sulfur concentration in the Finisher.

4. The fourth sets of lines are bolded and show the lowest sulfur concentrations. These lines show the simulation results of a 50% increase in the flux feeding rates combined with a doubling of the argon flow rates. The argon flow rates were increased from 17 scfm to 34 scfm in the Reducer and from 7 scfm to 14 scfm in the Finisher. Under these conditions, the sulfur of the steel in the Finisher returned to 0.008% within 7 minutes while the sulfur concentration of the steel that entered the Reducer continued to increase.

The sulfur conversion of the combined refining in the Reducer and Finisher increased from 84% during the initial steady-state operation to 90% after the return to 0.008% sulfur in the Finisher. These high conversion values indicate that the system of continuous reactors approaches its limits of effectiveness by removing 0.072% sulfur while maintaining a production rate of 165 t/hr. A further conversion increase would require the decrease in production rate. On the other hand, the overall sulfur conversion was still at 82% during the simulation with no corrective actions, removing 0.066% sulfur as compared to 0.042% during the initial steady state period.

The slags of the Reducer and Finisher were close to CaS-saturation after the sulfur increased but before the flux feeding rates were increased, showing the ability to hold a higher sulfur concentration than during steady-state operations. The sulfur concentrations of the slags increased from 4.3% to 6.0% in the Reducer and from 3.1% to 5.0% in the Finisher while steady-state flux feeding rates were maintained. The slag compositions returned to their initial, steady-state sulfur concentrations after the flux feeding rates were increased by 50%. The CaO-SiO_2-Al_2O_3-MgO-S quinary phase diagrams in Figures 9 and 10 were calculated with FactSage to illustrate these sulfur concentration changes in the Reducer and Finisher slags respectively.

The gas phase (S, S_2, SO, SO_2) represents a large part of the sulfur-rich region in these phase diagrams. Sulfur was chosen as one input component because FactSage was not able to calculate a phase diagram that uses CaO and CaS simultaneously as input components. However, the regions of the phase diagrams in Figure 9 and 10 with low sulfur concentrations compare well to the Al_2O_3-CaO-CaS phase diagram in Figure 53 in the Slag Atlas[6]. It contains a similar straight CaS-saturation line that parallels the CaO-Al_2O_3 axis at comparable sulfur concentrations.

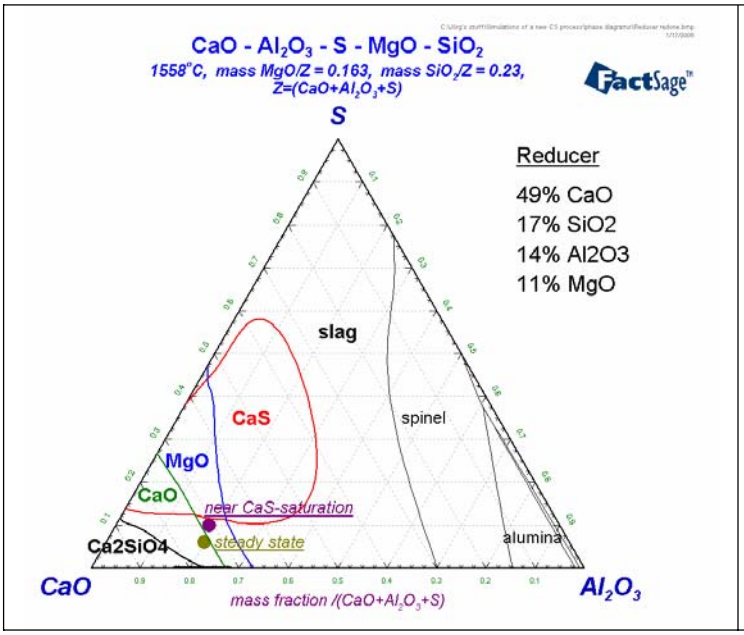

Figure 9: An increasing sulfur content of the **Reducer** slag is mapped on a CaO-SiO_2-Al_2O_3-MgO-S quinary phase diagram at 2836ºF. The sum of **CaO, Al_2O_3 and sulfides is 72%** of the total slag. The sulfur content of the slag increases from 4.3 % to 7.0%. The steel production (flow) rate is 165 t/hr.

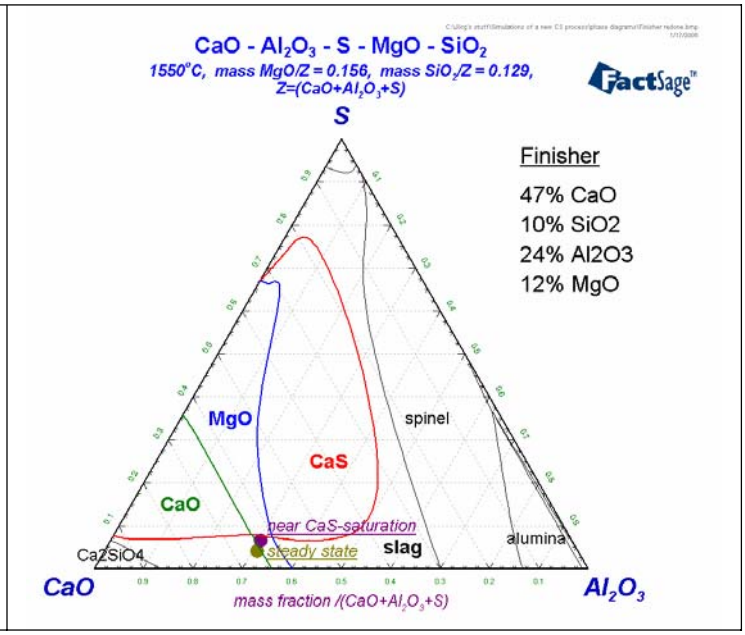

Figure 10: An increasing sulfur content of the **Finisher** slag is mapped on a CaO-SiO_2-Al_2O_3-MgO-S quinary phase diagram at 2822ºF. The sum of **CaO, Al_2O_3 and sulfides is 78%** of the total slag. The sulfur content of the slag increases from 3.1% to 5.0%. The steel production (flow) rate is 165 t/hr.

Simulation of a grade change decreasing manganese from 0.90% to 0.45%

The Metsim calculations of a grade change predicted that the concentrations of steel components can be changed during the operation of the continuous process without changing current tundish practices and amounts of intermix material. The grade change example involved the simulated decrease of the manganese concentration from 0.90% to 0.45% while keeping all other steel components constant. The simulation included a steady caster production of 165 t/hr.

In general, the grade change involves one closing and opening of each vessel (except the tundish) and the appropriate adjustments of alloys, fluxes, and scrap feeding rates. Details of the grade change are explained with four steps in Figure 11 and Table II. These steps are called “Alloy alteration”, “Batch operation”, “Finisher Refill”, and “Steady state return”. The changes of the Mn, C, and S in the steel of the Reducer and Finisher during the grade change are plotted in Figure 11. The operational changes as compared to the steady-state operation are summarized in Table II. The carbon concentration in the Reducer varied because the manganese alloys contain carbon (Table I). Varying residence times of the steel in the Reducer caused temporarily changes of sulfur concentrations.

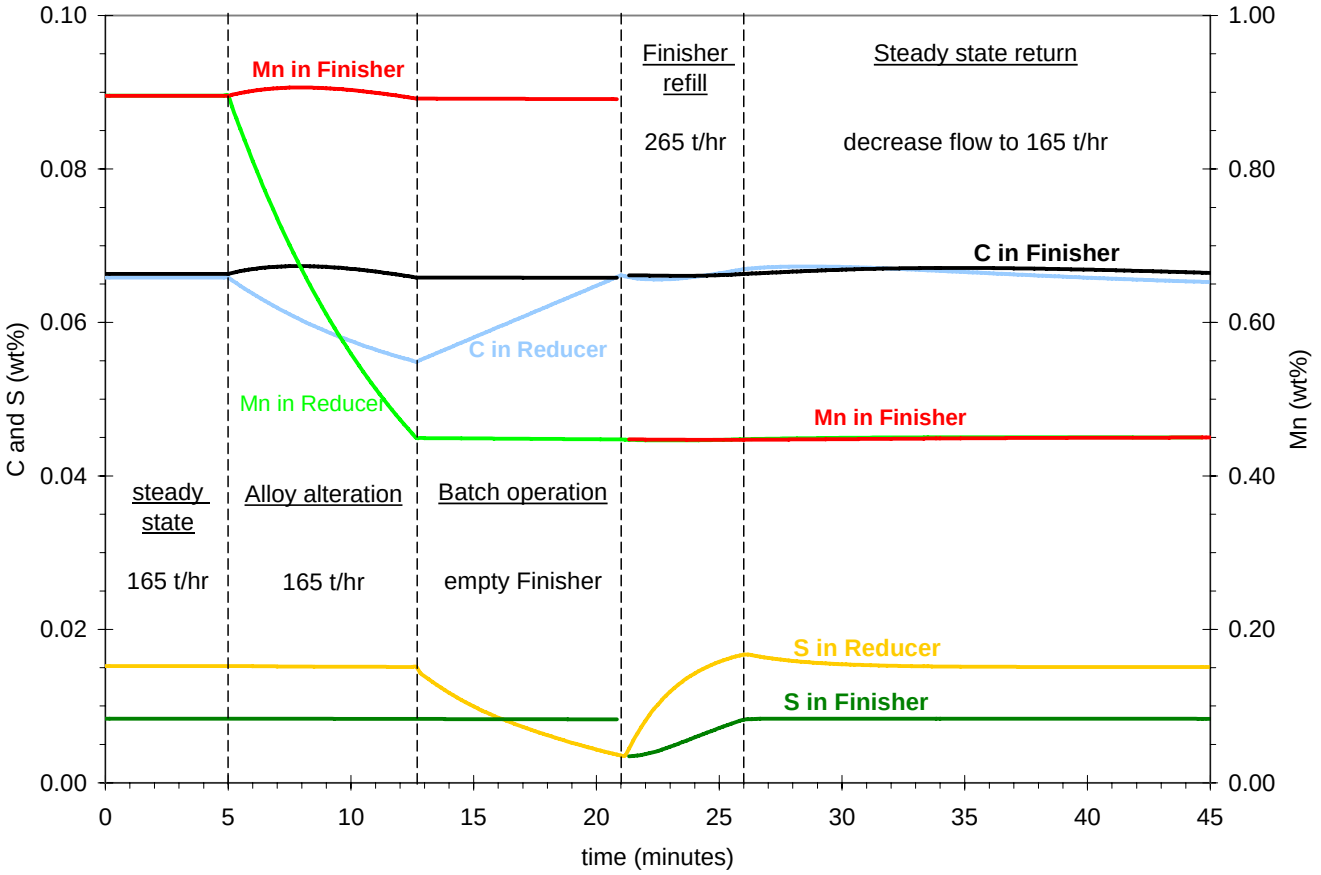

Figure 11: Calculated Mn, C, and S concentration changes in the steel of the Reducer and Finisher during a grade change are graphed.

Table II: The deviations of steel treatment and composition as compared to steady-state operation are summarized for a grade change that reduces the Mn concentration from a minimum of 0.90% to a maximum of 0.45%

Step	**Alloy alteration***	**Batch operation**	**Finisher refill**	**Steady state return**
Duration	8 min	8 min	5 min	15 min
EAF	none	4. Close slide gate 5. Slow scrap conveyer • Steel temperature and mass increase	14. Open slide gate 15. Flow steel at 265 t/hr 16. Increase scrap rate • Temp. & mass decrease	24. Return stepwise to 165 t/hr steel flow 25. Adjust steel level and temperature
Oxidizer	none	6. Close slide gate 7. Stop flux feeding	17. Open slide gate 18. Resume flux feeding rates • C increases	• C decreases
Reducer	1. Stop SiMn addition 2. Increase FeSi to 8.1 lbs/t • Mn decreases to new level • C & P decrease	8. Close slide gate 9. Decrease flux feeding rates to 1/3 10. Add a total of 3.4 lbs FeSi & 5.4 lbs carbon • C increases • S decreases	19. Open slide gate 20. Resume flux feeding rates 21. Start new alloys: 3.7 lbs/t SiMn, 7.1 lbs/t FeSi, 3.8 lbs/t HC-FeMn • S increases	26. Adjust time rate of alloy additions to steel flow
Finisher	3. Add 6.0 lbs/t MC-FeMn & 0.8 lbs/t HC-FeMn • Unchanged steel composition	11. Stop alloy additions and flux feeding 12. Remove most slag 13. Drain steel (possibly faster than 165 t/hr)	22. Close slide gate 23. Resume flux feeding rates • Mn is at new level • P & S are below spec. • S increases	27. Open slide gate 28. Adjust time rate of alloy additions to steel flow
Tundish	none	• Could increase steel mass	• Steel level lowers	• Refill to steady level

* The step "Alloy alteration" is not necessary if all alloys that are added in the Reducer need to be increased or stay unchanged.

The first 5 minutes in Figure 11 show the Mn, C, and S in the steel of the Reducer and Finisher at steady-state concentrations. During the next 8 minutes, the "Alloy alteration" step, the alloy additions and consequently steel concentrations were changed in the Reducer and Finisher. The SiMn addition was replaced with an increased FeSi addition in the Reducer, causing a decrease of the Mn as well as C and P concentrations in the steel since these three elements are components of the SiMn alloy (Table I). The increase in FeSi addition was required to maintain a consistent silicon concentration at all times. During the same "Alloy alteration" step, MC-FeMn and HC-FeMn were added in the Finisher to maintain the chemistry of the current grade.

The increase followed by a decrease of manganese and carbon concentration in the Finisher during the "Alloy alteration" step originated from a constant alloy addition rate of 6.0 lbs/t MC FeMn & 0.8 lbs/t HC FeMn during this period. Initially, the alloy concentrations increased by 0.01% Mn and 0.001% C because the incoming steel still contained large amounts of Mn and C. Both concentrations decrease to their original value as these components are diluted in the Reducer, changing the composition of the steel that entered the Finisher. Carbon is not adjusted in the Reducer during "Alloy alteration" because it is less costly to use high-carbon FeMn in the Finisher and because the carbon recovery with ferroalloys is more predictable.

The "Alloy alteration" step is not necessary if all alloys that are added in the Reducer need to be increased or stay unchanged. It does not matter if the alloy concentrations in the Finisher need to be increased or decreased (e.g. V or Nb) because the old grade will be drained before the Finisher will be refilled with the new grade.

During the "Batch operation" step, the flow from the EAF, Oxidizer, and Reducer are stopped and alloy additions and flux feeding are discontinued in the Oxidizer and Finisher. The stopping of the flow from the EAF also requires the slowing of the scrap conveyer. It is believed that the conveyer should continue to supply scrap to the furnace (at a slower rate) and the furnace steel mass and temperature should be increased during "Batch operation". This practice would allow an increased flow and scrap feeding rate during "Finisher refill". However, the EAF temperature increase, steel level, and the feasible scrap feeding rates would be best determined by the operators during actual operation.

The flux addition rates in the Reducer during "Batch operation" are decreased to one third of the initial steady-state addition rates to ensure a sufficient SiO_2 concentration in the slag, keeping the slag composition and the percentage of solid slag constant. Less SiO_2 is produced during this step than during steady-state operation because no oxygen-rich steel entered the Reducer. A one time addition of 3.4 lbs FeSi and 5.4 lbs carbon in the Reducer are necessary during "Batch operation". The silicon reduces the FeO that is generated during continued de-S of the steel due to continued flux addition and argon stirring. The carbon addition increases the carbon concentration to the required level.

The removal of most of the slag in the Finisher before draining and a continued (but possible decreased) argon flow rate would minimize the amount of entrapped slag as the Finisher is emptied. However, some slag cover needs to be maintained to protect the steel. The tundish mass could be increased by increasing the steel flow from the Finisher during "Batch operation", allowing a quicker return to the steady-state level at the end of the grade change.

The flow was discontinued from the Finisher once it was nearly empty, starting the "Finisher refill" step. The flow from the EAF, Oxidizer, and Reducer and the initial steady-state flux feeding rates in all reactors were resumed during the refilling of the Finisher. However, the steel flow through the first 3 vessels was increased to 265 t/hr to provide a full Finisher of the new grade within 5 minutes. A five-minute flow interruption for a grade change is similar to the time many companies would take to make ladle (or grade) changes at the continuous caster. The new grade contains the required lower manganese concentration and a lower phosphorus concentration. The phosphorus decreased from 0.008% to 0.006% because the alloy additions for the new grade, as listed in Table II, contained less phosphorus (Table I). The sulfur increased in the steel and slag of the Reducer and Finisher to its initial steady-state values after it was decreased during "Batch operation". The tundish level decreased until the Finisher was reopened. It is possible to fly the tundish at the end of the "Finisher refill" if required.

The grade change simulation was concluded with the "Steady state return" step. This step starts with the opening of the Finisher, supplying the new grade to the tundish and refilling it. The flow rate through the system was stepwise decreased during the simulation, decreasing the flow first to 220 t/hr for 15 minutes to increase the tundish level before returning to the 165 t/hr steady-state steel production. The value and duration of the flow rates depend on the steel level in the tundish at the time the Finisher reopens. The steel level and temperature in the EAF as well as the time rates of the alloy additions need to be adjusted according to the prevailing steel flow rate until steady-state production is achieved.

Although a simulated grade change with a stepwise concentration change, resembling current ladle practices, was described for continuous steelmaking, it is possible to change the steel composition gradually between grades. The head-to-tail variations in a single slab could be controlled by spreading out the grade change over several slabs by gradually increasing or decreasing the alloy additions. This practice could decrease the yield losses over current practices.

Simulated refractory temperatures of walls from a 124-ton ladle and a 27-ton continuous refining vessel

The thermal performances of the continuous refining vessels and of ladles were calculated and compared to predict differences between heat losses during continuous steelmaking and heat losses during current ladle operations. The calculated heat losses and steel temperatures are based on the wall designs illustrated in Table III. The walls of a ladle and the walls of a new refining vessel contain a 9-inch MgO-C working lining brick, a 3.15-inch chamotte back-up lining brick, and a 1-inch structural steel shell. In addition, the wall of a continuous refining vessel contains a 2.75-inch insulation brick between the back-up lining and the outer steel shell to minimize heat losses. The first row in Table III repeats the thickness of the layers in inches. The cells in the heat transfer model as well as the wall thickness in centimeters are illustrated in the second row of Table III. The overall thickness of the ladle walls is 13 inches or 33 centimeters while the walls of continuous refining vessels have an overall thickness of 15.75 inches or 40 centimeters.

The wall temperatures are higher in the walls of the new refining vessels as compared to ladle walls due to the additional 2.75-inch insulation brick. The calculated refractory temperatures of ladle and Reducer walls are plotted in Figure 12 as a function of distance from the working lining surface. The wall temperatures of the Reducer range between the values of the straight wall and of the exit-pipe wall. The calculated heat losses (fluxes) are higher through a ladle wall as compared to the walls of the Reducer. The bases of the calculations are steady-state and transient thermal models that are described in the next sections.

Table III: Illustration of the ladle and of the refiner wall designs including the 1-cm space steps in the thermal models

9 inches							**3.15** inches							**2.75** inches			**1** inch		
0	1	2	**	21	22	23	24	**	30	31	32	**	37	38	39	40	air		
Wall design of a typical ladle																			
working lining							back-up lining							shell			air		
Wall design of continuous steelmaking refining vessels																			
working lining							back-up lining							insulation brick			shell		air

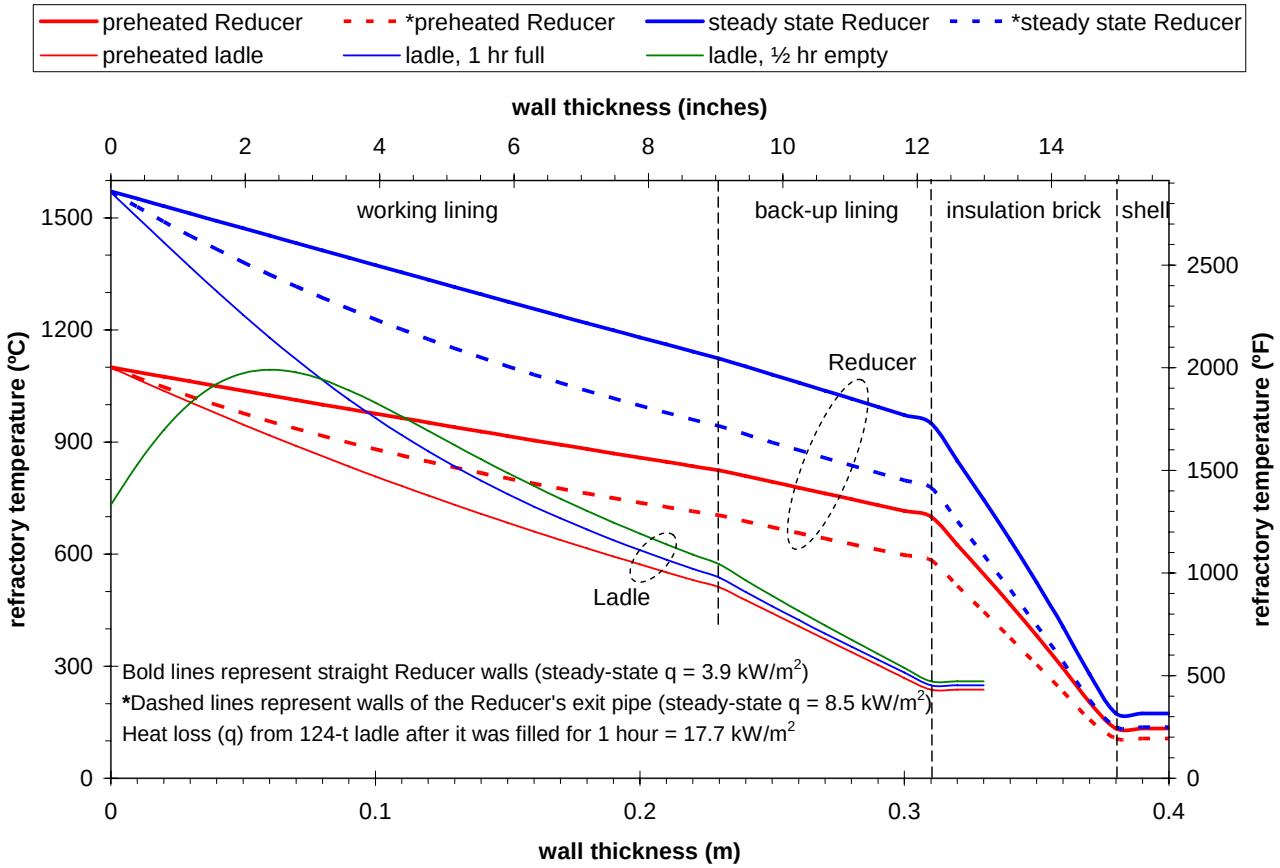

Figure 12: Temperature profiles and heat losses (fluxes) of a ladle wall and Reducer walls are compared

Steady state heat losses

Steady-state temperatures were calculated with Equation 3, using iterations and an estimated value of the inside wall temperature (working lining surface). The calculations were completed when the heat flux values and the outside surface temperature values (steel shell) converged with their estimates, which were adjusted during the iterations. Tolerated differences were smaller than 0.1 W/m^2 and 0.1ºC respectively. It was necessary to start the calculations with an estimated outside surface temperature because the heat transfer coefficient and the thermal conductivity are a function of temperature. Equation 4 was used to calculate the steady state surface temperature of the structural shell. The heat transfer coefficient was calculated with Equation 5, using an emissivity of 0.9 for the steel shell.

The equations of the thermal conductivity and heat capacity as well as the values of the densities for the different refractory materials of the walls are listed in the Appendix. It also includes the meaning of the variables and subscripts that are used for the heat transfer calculations (Equations 3 through 24).

$$T_n = T_{n-1} - \frac{qr_{inside}}{k_{n-1}} \ln\left(\frac{r_n}{r_{n-1}}\right) \text{ in Polar coordinates} \quad \text{or} \quad T_n = T_{n-1} - \frac{q\Delta x}{k_{n-1}} \text{ in Cartesian coordinates} \tag{3}$$

$$T_S = \frac{T_{air}}{\left(1 + \frac{k_S}{h_S \Delta x}\right)} + \frac{T_{S-1}}{\left(1 + \frac{h_S \Delta x}{k_S}\right)} \tag{4}$$

$$h = \varepsilon\left(\frac{5.7 * 10^{-8} W}{m^2 K}\right)\frac{\left(T_S^4 - T_{air}^4\right)}{\left(T_S - T_{air}\right)} + \frac{8.6W}{m^2 K} \tag{5}$$

The temperature changes due to additions and reactions in each refining vessel were calculated with Equation 6. The required enthalpy change was calculated with FactSage. The amount and type of alloy additions considered are reported in Figure 3 and the amount and type of flux additions considered are reported in Figures 5 and 6. The temperature losses due to these additions and associated reactions are 34ºF (19.0ºC) in the Oxidizer, 18ºF (10.0ºC) in the Reducer, and 8ºF (4.3ºC) in the Finisher. The total temperature loss due to additions and reactions in the three refining vessels is 60ºF (33.3ºC). In comparison, the average temperature effect of deoxidation and additions during current ladle treatment[5] are a loss of 54ºF (30ºC).

$$\Delta T = \frac{\Delta H}{mC_{p\_steel}} \tag{6}$$

The calculations of the total heat loss from the steel in each vessel required the determination of the surface area for each refining vessel. The shapes of the three refining vessel can be seen in Figure 1. More details of the vessel designs may be found in Figures 5, 6, and 7 in reference 1. The total working lining surface area of each refining vessels as well as the areas and shapes for different wall sections are listed in Table IV. The wall sections were simplified in order to minimize their number and the amount of computations.

Table IV: Documentation of the working lining surface areas for each simplified vessel section

	Oxidizer		*Reducer*		*Finisher*	
Section name	**Section area**	**Section shape**	**Section area**	**Section shape**	**Section area**	**Section shape**
upper vessel	11.80 m^2	r_{inside} = 0.75 m	6.90 m^2	r_{inside} = 1.00 m	12.60 m^2	r_{inside} = 0.75 m
lower vessel			7.60 m^2	r_{inside} = 0.65 m		
entry / exit	6.70 m^2	r_{inside} = 0.40 m	6.70 m^2	r_{inside} = 0.40 m	2.90 m^2	r_{inside} = 0.40 m
exit pipe	1.60 m^2	r_{inside} = 0.20 m	2.20 m^2	r_{inside} = 0.20 m	-	-
top / bottom / faces	3.90 m^2	straight	3.70 m^2	straight	3.60 m^2	straight
within vessel	2 x 0.70 m^2	inside / straight	2 x 0.90 m^2	inside / straight	-	-
Total area	25.40 m^2		28.90 m^2		19.10 m^2	

The heat flux of each wall section was calculated with Equation 7. The total heat loss from the steel was calculated with Equation 8 by summing the products of the heat flux and the areas assigned to each vessel section.

$$q = \frac{(T_0 - T_1)k}{\Delta x} \tag{7}$$

$$Q_{vessel} = \sum_{all\_sections}^{i} q_i A_i \tag{8}$$

The results of the steady-state heat loss calculations, as reported in Figure 13, indicate that the required EAF steel temperature, to maintain a constant Finisher steel temperature of 2822ºF, increases when the steel flow rate decreases, assuming that the steel would not be heated after it leaves the EAF. The estimated required EAF steel temperature would be 2900ºF at a production rate of 200 t/hr and 3000ºF at a production rate of 30 t/hr. The steady-state temperature losses from each vessel to the environment were calculated to range between 6ºF at 200 t/hr and 40ºF at 30 t/hr. The temperature losses due to additions and reactions, as calculated with Equation 6, were added to these values.

It was arbitrary chosen to set the upper limit of the EAF steel temperature at 3000ºF to minimize the wear on furnace equipment. As a result, the new process could operate as slow as 30 t/hr. Slow production rates support high chemical conversions due to long average residence times in each vessel. Correspondingly, the upper limit of the production rate, estimated to be 220 t/hr, would be determined by the required chemical conversion (and not by heat losses).

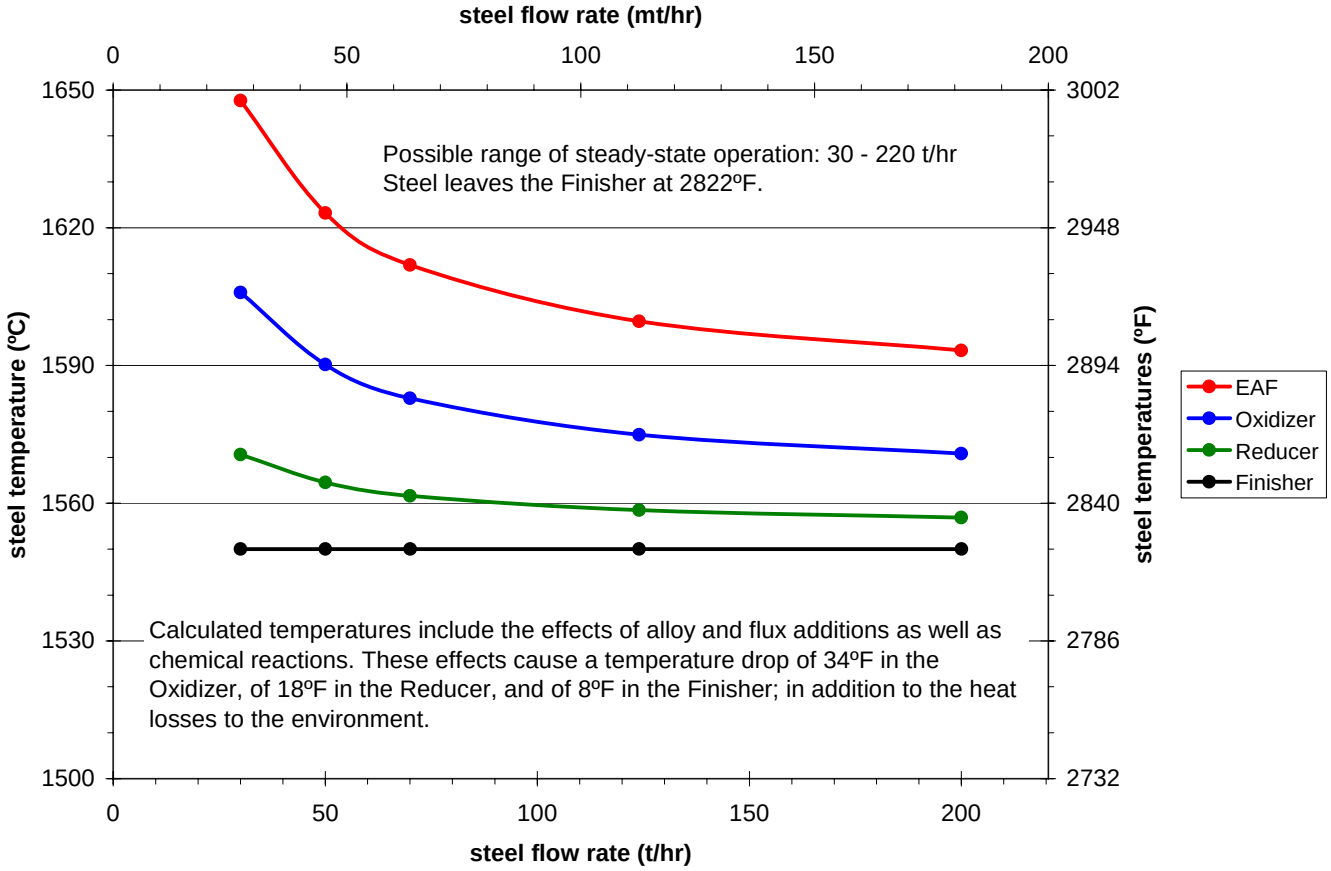

Figure 13: Calculated steady-state steel temperatures in the EAF, Oxidizer, Reducer, and Finisher at production rates that range between 30 t/hr and 200 t/hr are reported. The calculations were based on a constant steel temperature in the Finisher (2822ºF) and they include the effects of reactions and additions.

Transient heat losses during start-up

The transient heat transfer is governed by the parabolic diffusion or heat flow equation. Equation 9 lists the form of this equation in the Cartesian coordinate system. This form is needed for a straight wall.

$$\alpha \nabla^2 T = \frac{\delta T}{\delta t} \tag{9}$$

Equation 8 is the Cartesian finite difference form of Equation 10 for one spatial dimension and time.

$$T_{new\_n} = T_n + \left(\frac{k(\Delta t)}{\rho C_p (\Delta x)^2} \right) (T_{n+1} - 2T_n + T_{n-1}) \tag{10}$$

The transient heat flow equation as written with Equation 11, using the polar coordinate system, is needed for a curved wall.

$$\alpha \left[\frac{\delta^2 T}{\delta r^2} + \frac{1}{r} \frac{\delta T}{\delta r} \right] = \frac{\delta T}{\delta t} \qquad \text{or:} \qquad \alpha \frac{1}{r} \frac{\delta}{\delta r} \left(r \frac{\delta T}{\delta r} \right) = \frac{\delta T}{\delta t} \tag{11}$$

Equation 12 is a 1-D, transient, polar, finite difference heat flow equation. It has an additional term in the second parentheses as compared to Equation 10. The space steps (Δx and Δr) are 1 cm in both coordinate systems.

$$T_{new\_n} = T_n + \left(\frac{k(\Delta t)}{\rho C_p (\Delta r)^2} \right) \left(T_{n+1} - 2T_n + T_{n-1} + \frac{\Delta r (T_{n+1} - T_{n-1})}{2(r_{inside} + n\Delta r)} \right) \tag{12}$$

Equations 10 and 12 needed to be modified for the two cells that represent the boundary between two materials. These cells are cell 23 in Table III for the boundary between working lining and back-up lining and cell 31 for the boundary between back-up lining and insulation brick. Equation 13 shows the modified form of Equation 12.

$$T_{new\_n} = T_n + \left(\frac{k_n (\Delta t)}{\rho C_p (\Delta r)^2} \right) \left(\left(\frac{k_{n+1}}{k_n} \right) (T_{n+1} - T_n) - T_n + T_{n-1} + \frac{\Delta r (T_{n+1} - T_{n-1})}{2(r_{inside} + n\Delta r)} \right) \tag{13}$$

The surface temperature is calculated with Equation 14 in the cell that represents the steel shell and is next to the back-up lining (cell 31 for a ladle) or insulation brick (cell 38 for a refining vessel). The heat transfer coefficient was calculated with Equation 5. The temperatures in the two shells that represent the outer steel shell of the container (as illustrated in Table III) were set equal to the surface temperature calculated with Equation 14, assuming a zero temperature gradient within the outer structural steel shell.

$$T_{new\_S} = T_S + 2 \left(\frac{k(\Delta t)}{\rho C_p (\Delta x)^2} \right) \left[T_{S-1} - T_S - h \frac{\Delta x}{k} (T_S - T_{air}) \right] \tag{14}$$

The Fourier number (Equation 15) is needed to define the stability criterion. Equation 16 describes the stability criterion for the Cartesian and Polar finite difference form of the 1-D transient heat flow equation. The calculation of the surface temperature that includes the heat transfer coefficient requires Equation 17 to hold true for stable transient heat flow calculations.

$$Fo = \frac{\alpha(\Delta t)}{(\Delta x)^2} \tag{15}$$

$$Fo \leq \frac{1}{2} \tag{16}$$

$$Fo \leq \frac{1}{2\left(1 + h\frac{\Delta x}{k}\right)} \tag{17}$$

Equation 17 requires the Fourier number to be smaller than 0.5 (Equation 16). The maximum allowable Fourier number ranges between 0.2 at high wall temperatures with a heat transfer coefficient of 300 W/(m^2K) and 0.5 at low wall temperatures. The actual Fourier numbers during the simulation of the transient heat flow through the refractory lining was below 0.1 at high temperatures and below 0.2 at low temperatures.

The stability criterion as written with Equation 17 is needed to determine the time (Δt) and space (Δx or Δr) steps during the finite difference calculations. It was preferred to choose 10 seconds for the time step (Δt) because a time step of 10 seconds was already used during the dynamic Metsim simulations. The largest thermal diffusivity of the working lining does not exceed $2*10^{-6}$ m^2/s at room temperature. As already noted, the largest allowable value of the Fourier number is 0.2 at high temperatures. A space step (Δx or Δr) of one centimeter was calculated with Equation 18 based on these considerations.

$$\Delta x = \Delta r \geq \sqrt{\frac{\alpha(\Delta t)}{Fo}} = \sqrt{\frac{\left(2*10^{-6}\,\frac{m^2}{s}\right)(10s)}{0.2}} = 0.01m \text{ or 1 cm} \tag{18}$$

The transient heat flow model assumes that the temperature of the entire working lining surface (including the surface above the slag in the vessels) equals the instantaneous steel temperature. It was judged that this conservative assumption is reasonable when the refining vessel is filled with steel because it was calculated that the working lining surface above the slag is at an approximately 180ºF lower temperature than the steel, corresponding to an actual lower heat loss through this part of the reactor than simulated. However, this assumption greatly deviates from reality during the filling process. As a result, a modified heat transfer model was used until the final steel height was reached.

The modified filling model assumes a simplified cylindrical vessel that is preheated to 2000ºF (1100ºC), has a bottom area equal to the Oxidizer or Finisher (1.77 m^2), and a vessel height of 5.09 m, representing the area of the original vessel except for the bottom area. At time zero, the bottom area is only in contact with the steel and the rest of the cylinder is heated by radiation. The vessel is filled at a constant flow rate until it is completely full (e.g. the steel contacts the entire wall area). The assumption of a completely filled vessel is not supported by the value of the steel density. However, this assumption agrees with the general model, which assumes that the entire refractory surface is at the steel temperature at the time the vessel is full, matching the two models at this time during the simulation.

The refractory surface temperature of the wall area that is not covered by steel was calculated with Equation 19 during the filling simulation. It was assumed that the emissivity and the viewing factor have a value of one, overestimating the heat loss from the steel.

$$T_{new\_0} = T_0 + 2\left(\frac{k(\Delta t)}{\rho C_p(\Delta r)^2}\right)\left(T_1 - T_0 + \left(\frac{\Delta r}{k}\right)\left(\frac{A_S}{A_W}\right)(\varepsilon F)\sigma\left(T_{steel}^4 - T_0^4\right)\right) \tag{19}$$

At the moment when the steel contacts the refractory that was exposed and preheated by the radiation, the temperatures of the wall cells were shifted by half a cell to the right (away from the working lining surface). Equation 20 was used to calculate the new temperatures, which are represented by open circles in Figure 14. This procedure was followed because the meaning of the first cell changed from refractory surface temperature to steel temperature at the time the steel level rose to the height of a specific surface cell. The steel temperature was calculated with Equation 21 in the first cell while the vessel was still being filled.

$$T_{new\_n} = \frac{T_{n-1} + T_n}{2} \tag{20}$$

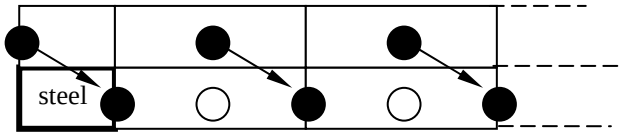

Figure 14: Illustration of the shift of temperatures within the modified filling model at the time the steel reaches the refractory

$$T_{0\_new} = \frac{T_0 m - \left(\sum_{covered\_areas}^{i} (T_0 - T_1)_i A_i \right) \left(\frac{\Delta t}{\Delta x} \right) \left(\frac{k_{wall}}{C_{p\_steel}} \right) + T_{0\_prev.vessel} \dot{m} - \left(\frac{\Delta t A_S}{C_{p\_steel}} \right) (\varepsilon F) \sigma \left(T_0^4 - T_{uncovered}^4 \right)}{m_{new}} \tag{21}$$

The steel was allowed to flow through the vessel once a vessel was full. At this time, the steel temperature was calculated with Equation 22, using the general heat transfer model. The steel temperature was calculated considering the heat flux and area from each vessel section (with different wall shapes) as well as the flow rate and the temperature of the steel that enters and leaves the vessel.

$$T_{0\_new} = \frac{T_0 m - \left(\sum_{all\_sections}^{i} (T_0 - T_1)_i A_i \right) \left(\frac{\Delta t}{\Delta x} \right) \left(\frac{k_{wall}}{C_{p\_steel}} \right) + T_{0\_prev.vessel} \dot{m} - T_0 \dot{m}}{m_{new}} \tag{22}$$

The transient heat transfer model was used to calculate the steel temperatures and the associated heat losses during the start-up of the new process. The simulation result in Figure 15 shows that the steel in the EAF would need to be superheated to 3068ºF before the furnace would be opened. The EAF steel temperature could be decreased to below 2950ºF eight minutes after the furnace opens, decreasing the power supply while supplying scrap. The steel temperature in the EAF would have to be continuously adjusted until it reaches its steady-state value of 2908ºF. These adjustments would be best controlled with continuous temperature measurements, possibly using available technology[9]. The steady-state steel temperatures of the EAF and of the three refining vessels that were reported in Figure 3 are plotted in Figure 15 with dashed lines.

The steel temperatures in the Oxidizer, Reducer, and Finisher would quickly decrease in accordance with the steel temperature in the EAF. The decrease of the combined heat losses from the steel in the Oxidizer, Reducer, and Finisher to the environment from a maximum of 2.5 MW during the filling process to a steady-state value of 0.4 MW is the cause of the decrease of the required EAF steel temperature. The simulations were performed to maintain a Finisher steel temperature of approximately 2822ºF at all times. Other simulation constrains included preheated refining vessels (2000ºF), a constant steel flow of 165 t/hr, the opening of each vessel as soon as it was filled, and no heating of the steel after it left the EAF. The temperature losses due to additions and reactions that were calculated with Equation 6 were included in the calculations.

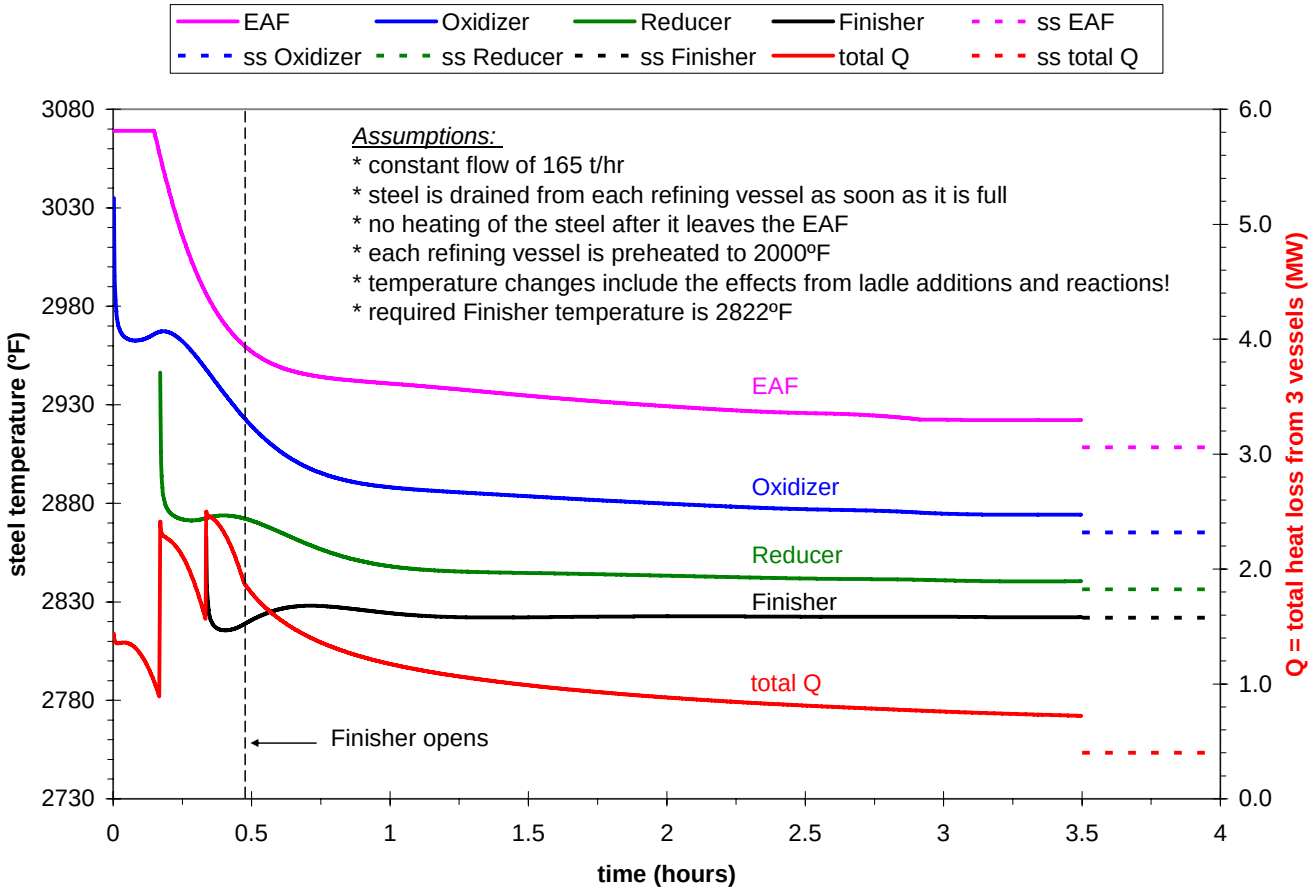

Figure 15: The calculated steel temperatures during the first 3.5 hours (solid lines) and during the steady-state operation (dashed lines), continuously producing 165 t/hr, are shown together with the combined heat losses from the three refining vessels (red lines).

Heat losses during ladle operations

The simulation of the heat losses from a ladle are based on a cylindrical vessel that can hold 124 tons of steel, is covered by a lid or an LMF roof, and has a total working lining surface of 45.90 m^2. The refractory area was divided into two sections. The section representing the top and bottom of the vessel was assumed to have the shape of a straight wall and a surface area of 10.70 m^2. The main vessel of the simulated ladle has an inner radius of 1.30 m and a surface area of 35.20 m^2.

The heat transfer through the lining of a ladle was calculated with the same equations that were used for heat transfer through the walls of the continuous refining vessels. The modified filling model was used for the first 4.2 minutes during the initial fill, simulating EAF tapping. Additional calculations as compared to the thermal simulations of the continuous refining vessels included the cooling of the hot inner surface of the working lining, which occurs after the ladle is emptied, using Equation 23. The corresponding heat transfer coefficient was calculated with equation 24. The viewing factor was estimated[10] to be 0.4 and the emissivity of the hot refractory was assumed to be 0.9.

$$T_{new\_0} = T_0 + 2\left(\frac{k(\Delta t)}{\rho C_p (\Delta x)^2}\right)\left[T_1 - T_0 - h\frac{\Delta x}{k}(T_0 - T_{air})\right] \tag{23}$$

$$h = F\varepsilon\left(\frac{5.7*10^{-8}W}{m^2K}\right)\frac{(T_0^4 - T_{air}^4)}{(T_0 - T_{air})} + \frac{8.6W}{m^2K} \tag{24}$$

The thermal calculations were repeated for 3 ladles, simulating a meltshop operation that produces 165 t/hr by tapping 124 tons every 45 minutes. The assumed schedule for these 3 ladles is summarized in the Table V. The ladles are only completely full during the one-hour period called “tap + LMF + transport”. The simulated ladles were allowed to empty over a 45-minute period called “casting”. The transport, cleaning, tap hole sanding, and preparing for the next heat was given 30 minutes during the period called "empty”.

The simulation results in Figure 16 indicate that the combined heat loss from these 3 ladles fluctuate between 1.3 MW at the time when one ladle is empty, one is full at the LMF, and one is being emptied at the caster and 6.0 MW when steel is tapped into one ladle, one ladle is transported to the caster, and one ladle is still being emptied at the caster. The calculated steel temperatures range between 3000ºF (tap temperature) and 2800ºF, which would be the temperature of the last steel that leaves the ladle. The calculated values do not include the temperature changes associated with heating, additions and reactions as well as radiation losses from uncovered ladles.

The initial heat loss during tapping into “ladle 1” at time zero in Figure 16 was 4.4 MW because the simulation included a preheated surface of 2000ºF, corresponding to the wall temperature profile “ladle preheat” in Figure 12. The initial heat loss during the successive taps was calculated to be 6.0 MW because the ladle wall was allowed to cool for 30 minutes. The corresponding wall temperature profile in Figure 12 (“ladle ½ hr empty”) shows that the working lining surface was calculated to be 1350ºF before the ladle was refilled, causing the increased heat loss during tapping. The peak heat loss during tapping slightly declined over time due to the soaking of the refractory. The average heat loss from the 3 ladles is 2.5 MW.

Table V: The schedule for using three 124-ton ladles during a 165 t/hr conventional production is illustrated.

hours	0.25	0.5	0.75	1	1.25	1.5	1.75	2	2.25	2.5	2.75	3	3.25	3.5	3.75	4
ladle 1	tap + LMF + transport				casting			empty		tap + LMF + transport				casting		
ladle 2	cast.	empty			tap + LMF + transport			casting			empty			tap + LMF + transport		
ladle 3	tran.	casting			empty			tap + LMF + transport			casting			empty		tap

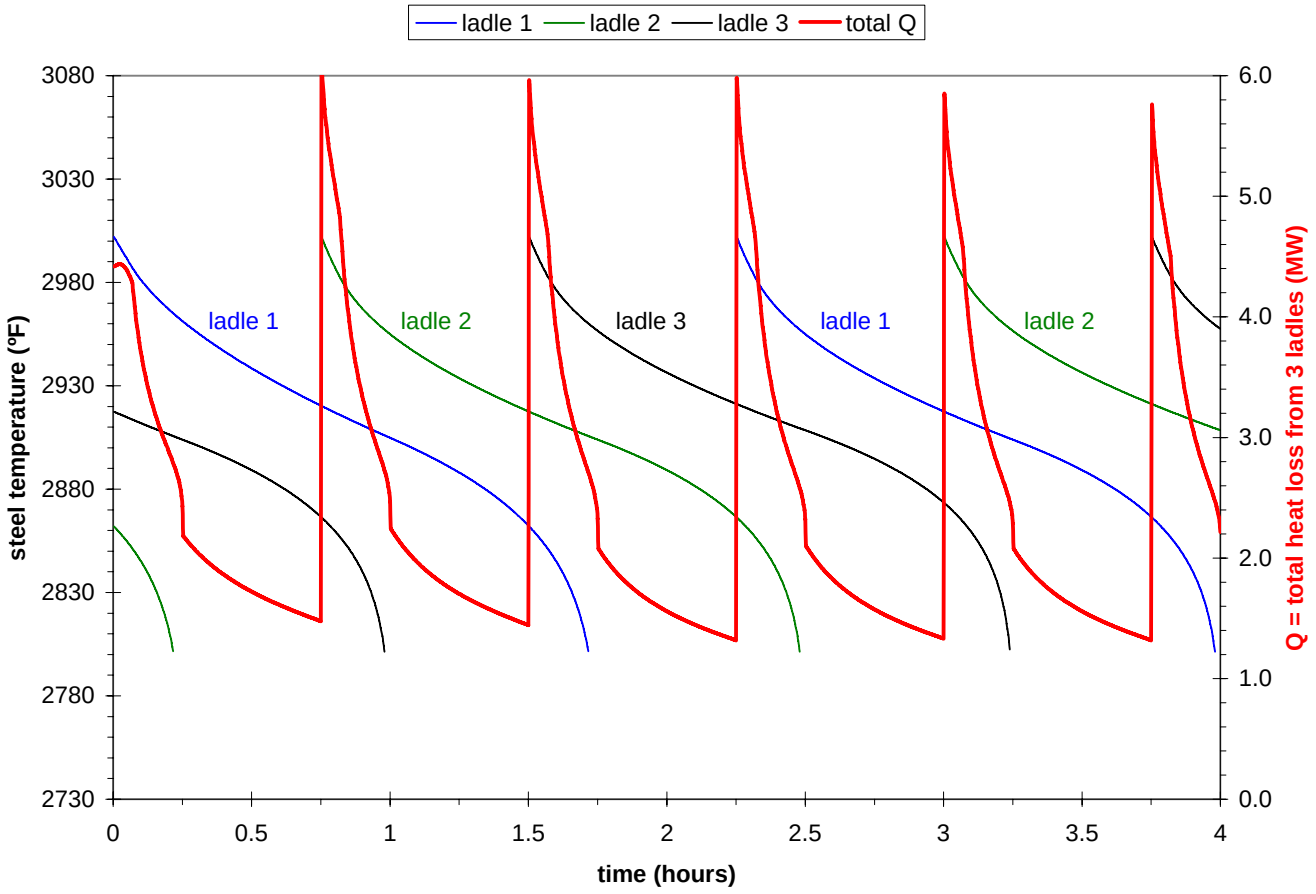

Figure 16: The steel temperatures in 3 ladles and the total heat loss from these 3 ladles are summarized. The steel production is 165 t/hr, tapping 124 tons of 3000ºF steel every 45 minutes in one of the ladles.

Comparing heat losses during ladle operations and during start-up of new continuous process

The calculated combined heat losses from the three refining vessels during the start-up of the continuous process and during steady-state operation are compared in Figure 17 to the calculated combined heat losses from 3 ladles during conventional operation. A production rate of 165 t/hr was assumed for both types of operation. The calculations predict that the heat losses from the three new refining vessels are lower than the average heat loss from 3 ladles. In fact, the value of the heat losses from the new refining vessels only reached the 2.5-MW average heat loss from the ladles at the moment when the steel first started to flow into the Finisher. The steady-state heat loss from the 3 new refining vessels is only 16% of the average heat loss from the 3 ladles.

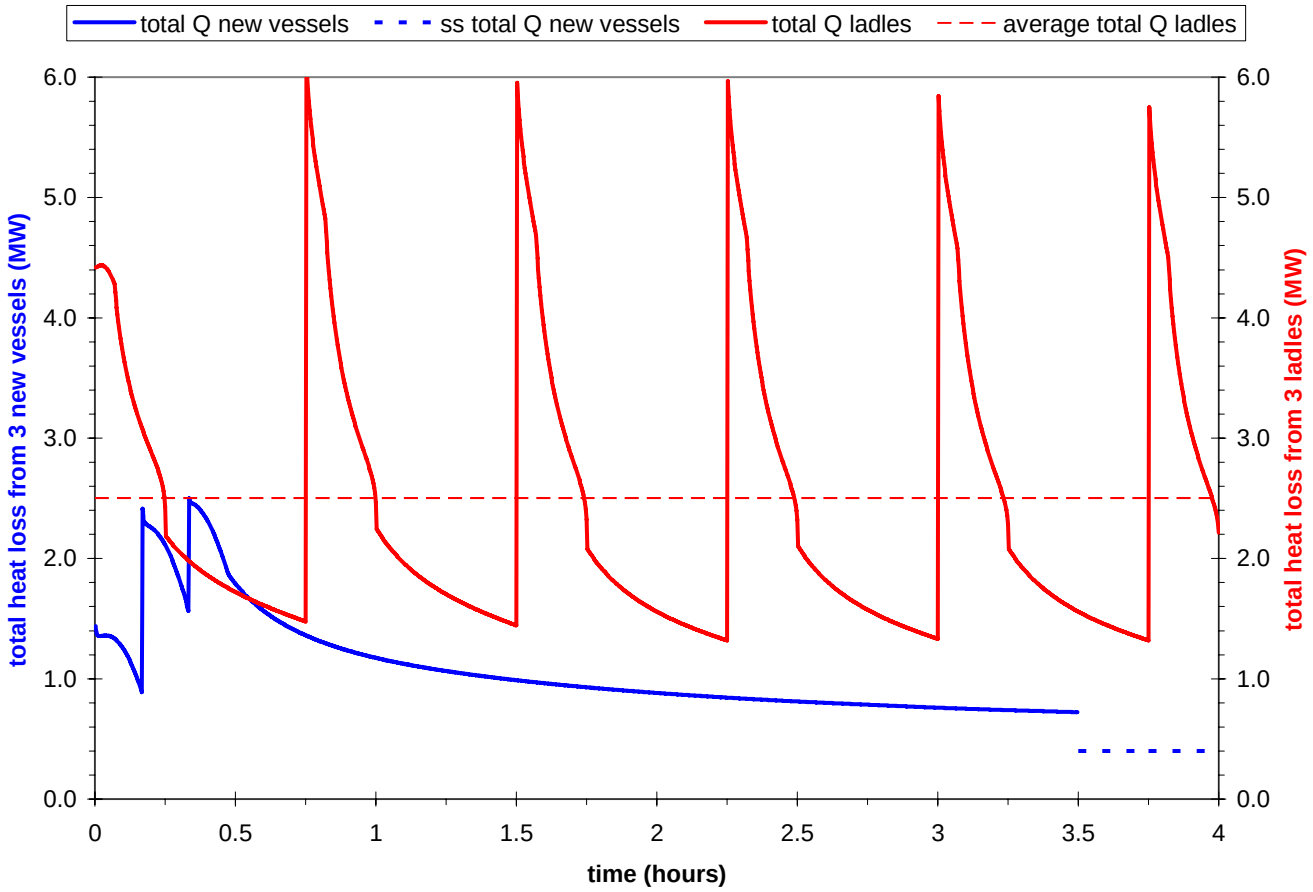

Figure 17: The calculated combined heat losses from the Oxidizer, Reducer, and Finisher over the first 3.5 hours of operation and during steady-state operation are compared to the calculated combined heat losses from 3 ladles, producing 165 t/hr in either case.

The general reasons for the decreased heat losses from the new refining vessels as compared to the ladles include a larger combined surface area of the ladles (135 m^2) as compared to the new refining vessels (70m^2), a longer turn-around time for the ladles (2.25 hrs) as compared to the combined average residence time in the new reefing vessels (28 min), and the heat loss from the refractories every time the ladles are emptied, which needs to be supplied by the next heat. In addition, the refining vessels are insulated with an additional 2.75-inch brick as compared to the ladles. This extra insulation is possible because the increased wall thickness and the additional vessel weight can easily be tolerated since the new refining vessels are small and compact and do not need to be moved on a regular basis.

It was estimated that the decreased heat losses would result into 10 kWh/t energy savings in the EAF due to lower tap temperatures, 2908ºF at steady state as compared to 3000ºF, and shorter residence times (equivalent to tap-to-tap times). The possible elimination of steel heating after EAF processing would accrue an additional savings of 30 kWh/t, based on current energy usage during LMF refining[5].

COST AND BENEFIT ANALYSIS

The savings from operating the continuous steelmaking process as compared to conventional EAF-LMF steelmaking would originate from yield increase, improved refining, and increased efficiency. The possible savings as summarized in Table VI are based on a current meltshop cost of $280/t that includes a scrap cost of $180/t but not the costs associated with a continuous caster.

Table VI: Estimated savings during the continuous steelmaking operation as compared to conventional EAF-LMF operation

	Savings ($/t)	Items	Short explanation
	8.50	4% metallic **yield increase** from 90% to 94%	Less FeO, more C in EAF; less oxidation, spills, heels
	2.50	50% decreased usage of reductants (Al, FeSi, etc.)	No carry-over slag, less reoxidation, cleaning, heels
	1.00	5% decreased usage of alloys & use more HC alloys	Less trimming, steady composition, de-C in Oxidizer
	1.25	Decreased usage of materials, e.g. fluxes, refractories	Steady-state, less FeO, more utilization, no cycling
Subtotal	**4.75**	**Improved refining**	
	3.15	Electricity savings of 70 kWh/t (& other utilities)	Decreased processing time, temperatures, heat losses
	2.20	Decreased use of electrodes and natural gas	Shorter processing, no LMF, decreased burner usage
	(-2.10)	Increased usage of carbon from 30 to 60 lbs/t	Foamy slag is required at all times
	(-0.35)	Increased gunning from 1 to 2 lbs/t	Constant contact between slag and refractory
	4.50	Decreased man-hours / ton from 0.60 to 0.45	Faster operation, less equipment and production steps
	(-0.60)	Increased usage of consumables, e.g. probes	More frequent (or continuous) measurements
Subtotal	**6.80**	**Increased efficiency**	
Total	**20.05**	based on $280/t current meltshop cost, including $180/t scrap cost but without casting cost	

It is believed that the yield could be increased by 4% because the EAF would constantly operate at near-equilibrium conditions at higher carbon concentrations than currently practiced, decreasing the oxidation of metallics. The carbon could be increased in the EAF because additional de-C is possible in the Oxidizer. In addition, yield losses due to reoxidation, spills, ladle cleaning and heels would be substantial decreased. The $8.50/t savings from yield increase are based on scrap savings.

Furnace or other oxidized slags would not carry over into refining vessels that are steadily operated under reducing conditions, decreasing the usage of reductants by 50%. Steady-state operations at required steel compositions in each vessel, insignificant amount of FeO in the slags of the Reducer and Finisher, and less reoxidation and air entrapment would decrease the amount of trimming while cheaper high-carbon alloys could be used due to additional de-C in the Oxidizer. Fewer amounts of fluxes as compared to current operations would be used based on the simulations. Refractory could be conserved due to substantial decrease of thermal cycling and operations at lower temperatures than currently practiced while continuously utilizing the equipment.

Increased efficiency would lead to savings from less energy consumption, decreased use of electrodes and natural gas, as well as decreased man-hours per ton of steel. The energy savings are based on a decrease of 70 kWh/t and a price of $0.045/kWh of electricity. The energy savings come from 10 kWh/t savings in the EAF and 30 kWh/t savings due to no heating after EAF processing as was discussed earlier. In addition, 10 kWh/t savings would accrue from 4% increased yield and 20 kWh/t from decreased auxiliary energy. The 20 kWh/t auxiliary energy savings are based on the average current auxiliary energy consumption of approximately 100 kWh/t[11]. The auxiliary energy savings would originate from less crane operations, decreased vessel transport, less preheating of vessels, and decreased maintenance of a smaller meltshop building and less equipment. The energy savings are illustrated with the schematic comparison of the processing times and steel temperatures of both process types in Figure 18. The figure is based on the hypothetical production schedule of 165t/hr with three 124-t ladles from Table V for the conventional practice and the results from the 165 t/hr chemical and thermal simulations of the continuous steelmaking process.

The savings from the decreased use of electrodes (1.0 lbs/t at $1.35/lb) and natural gas (100 scf/t at $0.0085/scf) is equalized by the increased cost due to doubling of the carbon consumption, assuming $0.07/lb of carbon. It is expected that more carbon but less natural gas would be consumed because the furnace would continuously operate with a flat bath. The constant contact between the slag and the refractory would possibly lead to an increased gunning consumption. An increased cost would be expected from increased chemical sampling either due to the use of continuous measurement technology or due to processing of more samples than currently practiced.

It is expected that the required man-hours could be decreased by 0.15 hr/t, saving $4.50/t if a labor cost of $30/hr is assumed. The decrease would originate from operations of fewer cranes, less vessel preparation, transport, and cleaning, less maintenance of a smaller meltshop and of less equipment, and a process that lends itself to increased automation. It is also expected that additional savings accrue from continuous improvements, especially during the first years of operation.

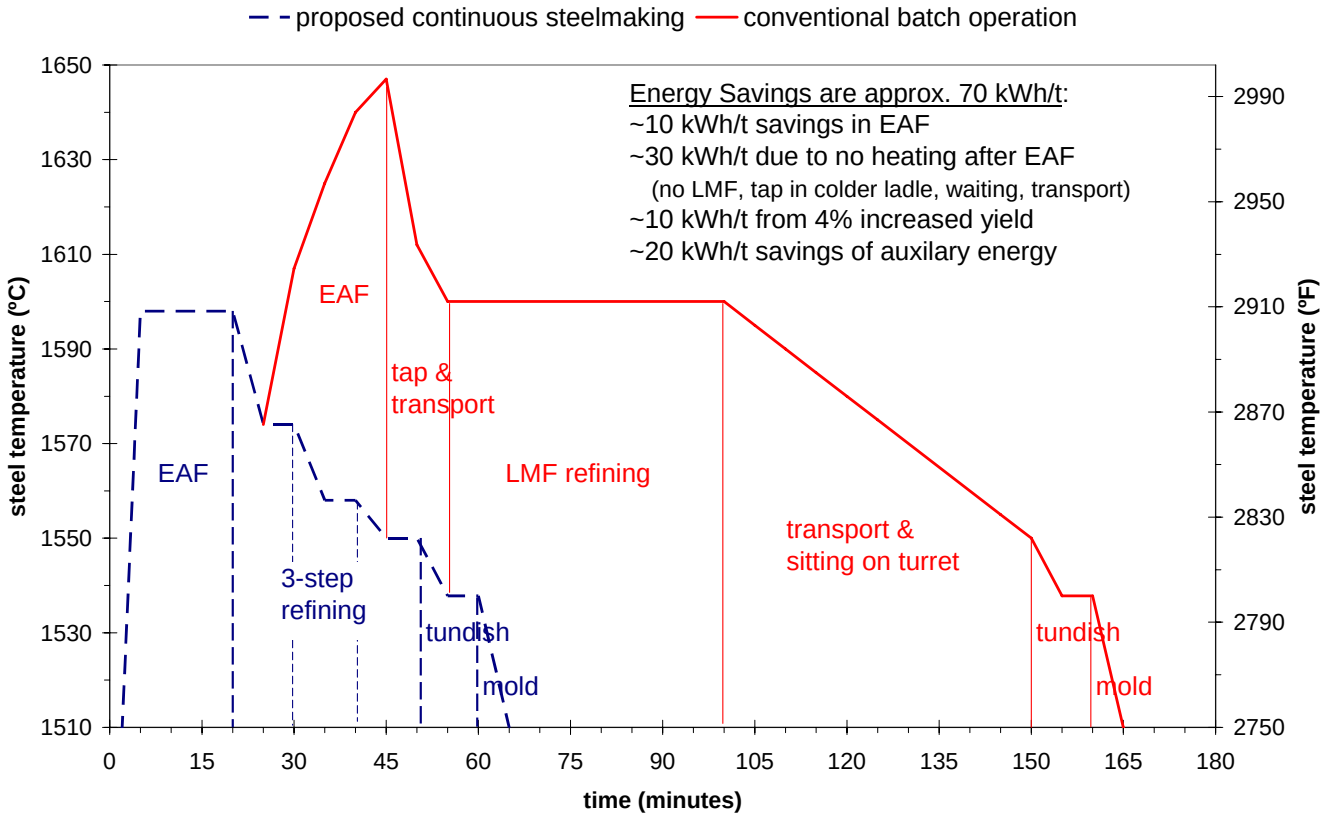

Figure 18: Schematic, simulation-based comparison of the temperature profiles of a 165 t/hr steel production using a conventional steelmaking practice and using the new continuous steelmaking process. Sources for energy savings are listed as well.

The estimated capital cost for equipment of a continuous steelmaking process producing 1,000,000 t/year is $35 million[12]. This equipment includes a 55-t AC Consteel® EAF with an 80 MVA transformer, a meltshop building with only one aisle, not counting caster aisle but including a maintenance area, 30 tons of structural support to support the equipment at the required height, material handling and hydraulic equipment, six refining vessels, nine slag pots, three transfer cars, and one non-contact twin plasma torch[13]. The estimated cost for conventional replacement equipment is $50 million[12].

The $15 million difference between the two estimates originate from the replacement of

- two aisles and crane tracks (furnace and LMF aisles) with one aisle and smaller cranes = $9.5 million savings
- one conventional 170-t EAF with one raised 55-t EAF, including conveyer = $2.0 million savings
- one LMF, its equipment, and six 150-t ladles with six 27-t refining vessels (2 sets) and a plasma torch = $3.5 million savings

The yearly operational savings of the continuous steelmaking process, assuming a one-million ton yearly production, would be $20 million dollars based on the estimates in Table VI. As a result, the payback period for the $35 million capital cost would be 1.8 years, corresponding to a rate of return on investment (ROI) of 57% as compared to current state-of-the-art equipment. It is expected that problems during the start-up of the unproven continuous steelmaking process would decrease the estimates of payback period and ROI.

SUMMARY

A new continuous steelmaking process has been designed in an effort to reduce meltshop costs and increase productivity beyond the possibilities of current EAF-LMF-CC meltshops. The performance of the new continuous steelmaking process was predicted with dynamic kinetic and transient thermal simulations. The calculated changes of the steel and slag compositions that would occur during a sudden sulfur increase in the scrap and during an abrupt grade change were based on steady-state simulations of a continuous 165-t/hr operation. It was discussed that continuous steel treatment could ensure that steel and slag compositions in the continuous reactors are consistently at their required aim composition without any necessary waiting period to achieve these compositions while standardized operations during conventional steelmaking are aimed to consistently meet the desired chemistry at the end of the ladle treatment.

The dynamic refining simulations included the calculation of the changes in steel and slag composition that would occur after the sulfur concentration of the incoming scrap is abruptly increased from 0.050% to 0.080%. The sulfur concentration in the Finisher (which is the equivalent of the final sulfur concentration during conventional ladle treatment) would slowly increase over a period of 40 minutes from 0.008% to 0.012%. No corrective actions were simulated during these initial 40 minutes of this upset. However, once corrective action (increased flux and argon stir) were applied to the process, the simulation predicted that the sulfur concentration in the Finisher (or final sulfur concentration) would rapidly decrease to its original value within 7 minutes. A production or flow rate of 165 t/hr was maintained at all times during the simulation.

The simulated grade change established that the concentrations of steel components could be changed abruptly during the operation of the continuous steelmaking process without changing current tundish practices and amount of intermix material while maintaining a steady caster production of 165 t/hr. The grade change example involved the decrease of manganese from 0.90% to 0.45% while keeping all other steel components at constant concentrations. The abrupt grade change includes one closing and opening of each vessel of the new process (except the tundish) and the appropriate adjustments of alloys, fluxes, and scrap feeding rates. The grade change procedure was explained with four steps that are called “Alloy alteration”, “Batch operation”, “Finisher Refill”, and “Steady state return”.

The results of the steady-state heat loss calculations indicate that the necessary EAF steel temperature would be 2900ºF at a production rate of 200 t/hr and 3000ºF at a production rate of 30 t/hr, assuming a constant steel temperature of 2822ºF in the Finisher. The transient heat transfer model calculated that the steel in the EAF would need to be superheated to 3068ºF before the furnace could be opened during the start-up of the new process if it is required not to heat the steel after it leaves the EAF and if the steel in the Finisher has to have a constant temperature of 2822ºF. The EAF steel temperature could be decreased to below 2950ºF eight minutes after the furnace would be opened due to the decrease of the combined heat losses from the steel in the three new refining vessels. The steady-state EAF temperature would be 2908ºF, assuming the 165 t/hr are continuously supplied to the tundish at a temperature of 2822ºF.

The simulation of the heat losses from 3 ladles, simulating a meltshop operation that produces 165 t/hr by tapping 124 tons of 3000ºF steel every 45 minutes, indicates that the combined heat loss of these 3 ladles averages 2.5 MW. The calculated maximum combined heat losses from the three refining vessels during the start-up are 2.5 MW, decreasing rapidly to the steady-state heat loss of 0.4 MW that is only 16% of the heat loss from the 3 ladles. The refractory temperatures are higher in the walls of the new refining vessels as compared to ladle walls due to the additional 2.75-inch insulation brick. It was estimated that the decreased heat losses would result in 10 kWh/t energy savings in the EAF and 30 kWh/t due to the possible elimination of steel heating after EAF processing. Increase yield and less auxiliary energy are sources of additional energy savings.

A cost analysis predicted that $20/t could be saved with the new continuous steelmaking process over current meltshop costs. The savings would primarily originate from a 4% yield increase, improved refining due to no carry-over slag and less oxidation, and increased efficiency due to less energy and material consumption as well as decreased man-hours per ton of steel. The capital cost for the new process was estimated to be $35 million or $15 million less than for conventional steelmaking equipment producing one million ton of steel per year. The predicted payback period is 1.8 years, corresponding to a rate of return on investment of 57%.

ACKNOWLEDGEMENT

This material is based upon work supported by the U.S. Department of Energy under cooperative agreement number DE-FC36-03ID14279. Such support does not constitute an endorsement by DOE of the views expressed in the article.

REFERENCES

1. Peter, J., Peaslee, K.D., Robertson, D.G.C., Zhang, L., Thomas, B.G. “Introduction of novel, scrap-based, fully continuous steelmaking process,” AISTech 2005 Proceedings, Vol. II, 2005, pp.623-634
2. Peter, J., Peaslee, K.D., Robertson, D.G.C., Thomas, B.G. “Experimental Study of Kinetic Processes during the Steel Treatment at two LMF’s,” AISTech 2005 Proceedings, Vol. I, 2005, pp. 959-973
3. Zhang, L., Aoki, J., Thomas, B.G., Peter, J., Peaslee, K.D. “Design of New Scrap-based Continuous Steelmaking Process using CFD Simulation,” ICS Proceedings - 3rd International Congress on Science and Tech. of Steelmaking, 2005, pp. 577-590
4. Aoki, J., Thomas, B.G., Peter, J., Peaslee, K.D., “Experimental and Theoretical Investigation of Mixing in a Bottom Gas-Stirred Ladle” AISTech 2004 Proceedings, Vol. I, 2004, pp. 1045-1056
5. Peter, J., Peaslee, K.D., and Robertson, D.G.C., “Study of Current Steelmaking Practices to Evaluate the Viability of Continuous Steelmaking,” 2004 AISTech Proceedings, Vol. I, 2004, pp. 1071-1084
6. Verein Deutscher Eisenhüttenleute (VDEh), “Slag atlas”, Verlag Stahleisen m.b.H., Düsseldorf, Germany, 1981
7. Turkdogan, E. T. “Fundamentals of Steelmaking” The Institute of Materials, London, UK, 1996
8. Roth, R. S., Negas, T., Cook, L. P. “Phase Diagrams for Ceramists Volume IV” The American Ceramic Society, Columbus, OH, 1981
9. Lagerberg, J. L., Oldenburg, W. W., Huisman, R. S., Yardy, J., Kendal, M. “Experience with a Novel Approach to Continuous Tundish Temperature Measurement” AISTech 2004 Proceedings, Vol. II, 2004, pp. 781-785
10. Poirier, D.R., Geiger, G.H., “Transport Phenomena in Materials Processing”, The Minerals, Metals & Materials Society, Warrendale, PA, 1994 (Fig. 11.15 p. 385)
11. Stubbles, J. “Energy use in the U.S. Steel industry: A historical perspective and future opportunities” US Department of Energy, September 2002
12. Cost estimates from Core Furnace Systems, July 13, 2005
13. Cost estimate from INDUGA GmbH & Co. KG, July 13, 2005

APPENDIX

Thermal conductivity, heat capacity, and density of refractories

Thermal conductivity of the working lining:	$k_{wl} = -(3*10^{-10})T^3 + (2*10^{-6})T^2 - (0.004)T + 4.5$	in W/(m*K)
Thermal conductivity of the back-up lining:	$k_{bl} = (0.0003)T + 1.5$	in W/(m*K)
Thermal conductivity of the insulation bricks:	$k_{insu} = (0.00015)T + 0.25$	in W/(m*K)
Heat capacity of all refractories:	$C_p = (9*10^{-9})T^3 - (2*10^{-4})T^2 + (0.577)T + 800$	in J/(kg*K)

The temperature (T) in above equations is expressed in degrees Celsius!

Density of the working lining:	$\rho_{wl} = 3000\, kg/m^3$
Density of the back-up lining:	$\rho_{bl} = 2200\, kg/m^3$
Density of the insulation bricks:	$\rho_{insu} = 1000\, kg/m^3$

Variables

α = thermal diffusivity = $\frac{k}{\rho C_p}$
δ = partial differential operator
ΔH = enthalpy change
Δr = space step (1 cm) in the Polar coordinate system (curved wall)
Δt = time step during one transient calculation (10 sec)
ΔT = temperature change
Δx = space step (1 cm) in the Cartesian coordinate system (straight wall)
ε = emissivity
ρ = density
σ = Boltzmann constant
∇^2 = Laplace operator

A = surface area of the working lining
C_p = heat capacity
d = diameter
F = viewing factor
Fo = Fourier number
h = heat transfer coefficient
k = thermal conductivity
m = steel mass in a refining vessel
$\dot{m}$ = steel flow between vessels
q = heat flux
r = radius
t = time
T = temperature

Subscripts

air = air properties
covered = working lining surface that is in contact with steel
i = counter of vessel sections
inside = location of inner working lining surface
n = current cell number
n+1 = current cell number minus one
n-1 = current cell number minus one
new = value after calculations during one time step
new_n = value of cell n after calculations during one time step
new_S = value of cell S after calculations during one time step
new_0 = value of cell zero after calculations during one time step
steel = steel properties
s = nominal top surface of steel bath
S = (quasi) surface cell 31 in ladle model and (quasi) surface cell 38 in continuous-refiner model
S-1 = cell S minus one
uncovered = working lining surface that has not been in contact with steel
vessel = value for one vessel
w = wall surface of uncovered working lining
wall = properties of the working lining
0 = cell zero representing the steel and the working lining surface
0_prev.vessel = properties of steel in the previous vessel
1 = first cell after cell zero